DEVELOPMENT OF A MICROBIAL FUEL CELL FOR ENERGY RECOVERY FROM WASTEWATER

By

Kabelo Mike Ledwaba

Submitted in accordance with the requirements for the degree of

MASTER OF TECHNOLOGIAE

In the subject

CHEMICAL ENGINEERING

At the

University of South Africa

Supervisor: Prof Bilal Patel and Prof Touhami Mokrani

October 2017

DECLARATION

Student number: 39448045

I, Kabelo Mike Ledwaba ,declare that all the work in the document **"DEVELOPMENT OF A MICROBIAL FUEL CELL FOR ENERGY RECOVERY FROM WASTEWATER"** is my own work and that all sources that I have used or quoted have been indicated and acknowledged by means of complete references. It has not been submitted before for any examination to any other University.

…… 20/10/2017…

(Signature of candidate) Date

DEDICATION

*To God, thank you for your love, guidance and wisdom. If it wasn't for you my God, I wouldn't be where I am today. "**You made a way**". To my mother (Mrs Jane Ledwaba) for encouraging us to go to school were indeed not in vain*

In addition, to my late father: Joseph Gaboile Seitlhamo

PRESENTATION AND CONFERENCES

Poster Presentation and Abstract

Kabelo Ledwaba: **Development of a Microbial Fuel Cell for Energy Recovery from Wastewater:** African Energy Material Conference (AEM) at CSIR Pretoria, 28-31/03/2017

Oral Presentation and Abstract

Kabelo Ledwaba: **Development of a Microbial Fuel Cell for Energy Recovery from Wastewater:** University of South Africa (UNISA) College of Science, Engineering and Technology. Postgraduate symposium 18 September 2015.

To be presented at the 5th Nano Today Conference (Nano Today 2017)

Microwave-hydrothermal synthesis of MnO_2 as electrocatalyst for Microbial Fuel Cell application. K. Ledwaba*, B. Patel, T. Mokrani; **Nano Today Conference - Conferences - Elsevier at Hawaii, USA (Waikoloa)_** December 6-10, **2017**

ACKNOWLEDGEMENTS

I would like to express my sincere gratitude to the following:

- Prof. Bilal Patel for accepting me to pursue this research under your supervision, your valuable advice, critical feedback and guiding me to the right direction. I truly appreciate the tremendous support
- I would also like to thank Prof. Touhami his guidance and assistance. You have encouraged me to always work hard and do better.
- I would like to also acknowledge all the suggestions that contributed to the success of this work from my fellow researchers
- I also thank Dr Isaac Beas and Dr Themba Tshabalala for helping me to be able to perform the BET and SEM measurement
- My thanks also go to all staff members of the Civil & Chemical Department for their support and encouragement
- I acknowledge the financial support from the Chemical industrial Education & Training Authority (CHIETA) and National Research fund (NRF).

I am grateful and deeply indebted to my wife (Betty) and my family for their continuous support, love and understanding throughout my studies

ABSTRACT

A key engineering challenge is a transition to cleaner sustainable energy supply that is derived from renewable resources. Furthermore, affordable access to this modern sustainable energy services for communities in particular poor rural and urban communities is crucial. Microbial fuel cell (MFCs) is an emerging renewable alternative technology with potential to be self-sustaining that could alleviate the energy crisis and reduce environmental pollution. The use of the MFC as a dual system for electricity generation and wastewater treatment is been well reported in literature.

Manganese dioxide (MnO_2) is an effective electro-catalyst that have been used for alkaline fuel cells and battery application. MnO_2 have a high conductivity and high structural porosity for ion and gas transport. In addition, MnO_2 have a favourable crystal morphology, which makes it particularly useful for improving oxygen reduction reaction in the fuel cell. Graphene (GO) will be loaded on MnO_2 surface as an effective support material. GO is a material good for electrical conductivity and their mechanical strength is applicable in electro-catalytic activities and is cost effective.

In this work, a constructed dual chamber MFC configuration with graphite rod electrodes, MnO_2-GO electrocatalyst and proton exchange membrane (PEM) using municipal sewage wastewater to generate electricity. The MnO_2 as an alternative electro catalyst used for oxygen reduction reaction (ORR) in the MFC while using reduced graphene (rGO) as a support to enhance electrode surface area. Also addressing the effect of graphene material loading on MnOx catalyst for electrochemistry. The characterization of the MnO_2-GO electrocatalyst have been analysed using X-Ray diffraction (XRD), Brunau-Emmett-Teller (BET) surface area and Fourier transform infrared spectroscopy (FTIR) for structural properties. Electrochemical techniques such as cyclic voltammetry (CV) for MnO_2-GO electrocatalyst. Thermal gravimetric analysis (TGA) for the thermal properties, and the morphological properties probed by Scanning Electron Microscopy (SEM).

The dual chamber MFC design functioned successfully and tested for energy generation from municipality sewage wastewater. The maximum voltage of 586 mV reached during MFC operation with various sewage municipal wastewater COD of 100-300mg/L. The maximum power density of 248 mW/m^2 with resistance of 16.98 Ω and highest current density of 1.72mA/m^2 was observed at the first cycle as compare to other cycle. The lowest value of 0.002159 mA/m^2 obtained at the end of 10 days. The content of municipality sewage wastewater is capable of generating electricity.

The physico-chemical properties of α-MnO_2 exhibits excellent cycling stability on the electrochemical. This excellent cycling stability of α-MnO_2 as a super capacitor electrode material. In addition, the graphene material loading on α-MnO_2 has improved the electro catalytic activity, which influences the kinetics of the reduction reaction. The α-MnO_2 synthesized BET analysis specific surface area of 134.61m^2 g^{-1} reported. MFC technology has the potential to finds its own niche in the energy industry as it is becoming more and more sustainable due to the lower cost of electro catalyst materials. Power densities of 248 mW/m^2 using wastewater with COD of 291mg/l were much higher than those previously obtained using low strength wastewater. These results have opened doors for further investigation of improving electro catalysis, utilized high concentration wastewater with high COD and improved MFC design including electrode materials.

TABLE OF CONTENT

List of Figures

List of Tables

ABBREVIATIONS

AC	Activated Carbon
AD	Anaerobic Digester
AFCs	Alkaline fuel cells
Ag/AgCl	Silver/Silver Chloride
BET	Brannauer-Emmett-Teller
BOD	Biological Oxygen Demand
CAS	Conventional Activated Sludge
C	Carbon
CE	Coulombic efficiency
CEM	cation exchange membrane
COD	Chemical Oxygen Demand
CO_2	Carbon Dioxide
CoTMPP	Cobalt-tetramethoxy-phenyl-porphyrin
C_n	Theoretical amount of coulombs
C_P	Actual amount of coulombs
Cu	Copper
CV	Cyclic voltammetry
DO	Dissolve Oxygen
DOE	Department of Engery
DMFs	Direct Methanol Fuel cell
EA	Electrons Aceptor
EDS	Energy dispersive X-ray spectroscopy
EEM	Exoelectrogenic Microorganisms
EIS	Electrochemical Impedance Spectroscopy
E_{emf}/EMF	Electromotive force
Ecell	Cell potential
E^0	Theoretical Cell voltage
E_{an}	Anode potential
E_{cat}	Cathode potential
EIA	Energy Investment Outlook

FePc	Iron phthalocyanine
FT	Fischer-Tropsch
FTIR	Fourier transform infrared spectroscopy
GAC	Granular Activated Carbon
GCE	Glassy Carbon electrode
GHG	Greenhouse gas
r-GO	Reduced graphene
GWh	Gigawatt hour
HRT	Hydraulic Residence Time
KBr	Potassium Bromide
K	Potassium
MCFCs	Molten carbonate fuel cells
MEA	Membrane Electrode Assembly
MFC	Microbial Fuel Cell
MnOx	Manganese Oxide
Mtoe	Megatoe
OCV	Open circuit voltage
ORR	Oxygen reduction reaction
OER	Oxygen evolution reaction
P	Power
Pmax	Maximum Power
PEM	Proton exchange membrane
Pt.	Platinum
PAFCs	Phosphoric acid fuel cells
R	Universal gas constant 8.314 J/mol-K
SEM	Scanning electron microscopy
SOFCs	Solid oxide fuel cells
T	Temperature
TW·h	Terawatt/hour
TEA	Terminal Electrons Acceptor
TGA	Thermogravimetric analysis

UCT	University of Cape Town
WWTP	Wastewater treatment plant
WRC	Water Research Council
XRD	X-ray diffraction

LIST OF SYMBOLS

F	Faraday constant
A	Ampere
G	Gibbs free energy
ΔG	Gibbs free energy
V	Volts
W	Watts
I	Current
IR	Internal Resistance
mS	Millesiemens
s	Second
h	Hour
Hz	Hertz
%	percent
^{o}C	degree Celsius
Pd	power density
W/m^2	i current density
mW/m	watt per square meter
Ω	Ohm
m^2	square metre
mL	millilitre
ml/min	millilitre per minute
g/L	grams per litre
cm	centimeter
µg	microgram
µl	microliter

CHAPTER 1

1 INTRODUCTION

This chapter highlights the environmental, economic and social needs for sustainable renewable energy and outlines the background, problem statement, aims and objectives of the proposed study, which focuses on microbial fuel cell (MFC).

1.1 Background

Economic development in the modern society is dependent on energy. The steady increase demand for energy and power application is greatly challenge globally and the constant sufficient supply of energy is required for economic growth. Any load shedding or interrupted on energy supply affects the economy and social welfare negatively [1]. According to United State, annual reports from The World Energy Investment Outlook 2014 (EIA2014) energy consumption and demands keeps on increasing (see Fig 1.1) [2]. Over centuries, the world has heavily relied on fossil fuels as energy, which includes coal, petroleum, and natural gas. Fossil fuels combustion yields carbon dioxide (CO_2) emission (greenhouse gas (GHG)) that contributes towards global warming and climate change. Rapid depletion fossil fuels reserves are under strain due to the high consumption rate of energy. This strain on energy sector (including government and companies) drive forces for alternative sustainable energy sources and technology to meet future energy demands [3].

South Africa's energy mix is characterised strongly dependence on cheap and abundantly available coal. More than 90% electricity is generated from coal-fired power station [4]. The growing population and rapid industrialisation increases pressure on power demand. The transition to green technologies that is economically and environmental friendly as alternative to generate electricity is in demand. Recently, lot effort has done on energy resources development and power generation technologies.

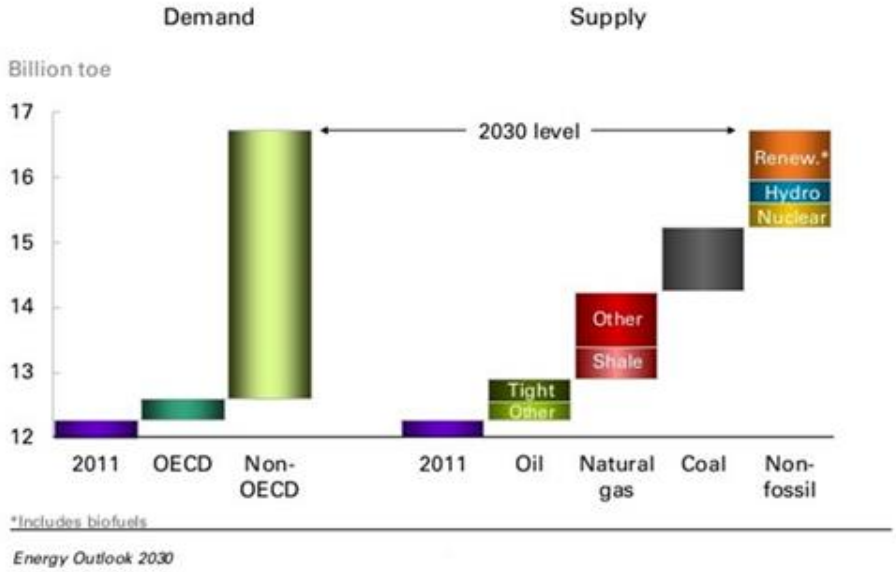

Figure 1.1 Schematic for energy demand over supply

1.2 Prospectus for renewable energy

The development of an alternative energy resource is a key to solve the energy crises and environmental challenges associated with fossil fuel. Trends shows that the solar, wind, tidal and geothermal energy are sustainable renewable energy sources, which addressing environmental impacts and energy demands. To maintain satisfactory growth levels, clean sustainable renewable energy sources and cost effective efficient technologies are the solution [5].

In South Africa (SA), the Department of Energy (DoE) is shifting the focus from fossil fuels towards alternative renewable energy. The target is to reduce coal's contribution for energy mix to 46% by 2030. The Department aims to achieve an energy mix consisting of 26 % renewable energy, 13% nuclear, 8% open cycle gas turbines, 3% pumped storage, 3% combined cycle gas turbines see in Fig 1.2 [6]. Clean sustainable renewable energy sources and technology can meet the growth demand of energy and reduce greenhouse gas emissions [7, 8].

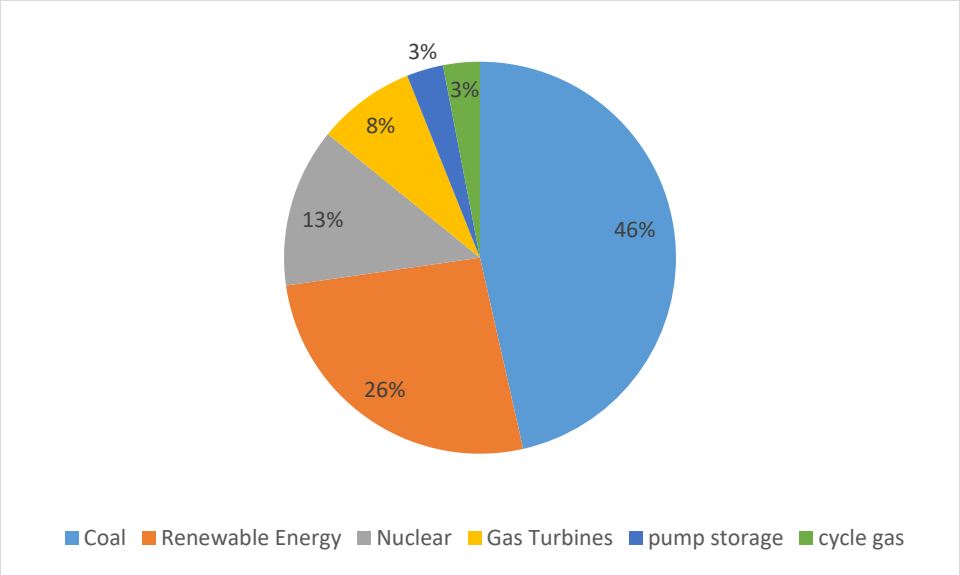

Figure 1.2. Proposed Energy Mix in South Africa for 2030

1.2.1 Energy generation source

Throughout the world, energy production requires water and the extraction, treatment and distribution of water requires energy. This inter-relationship between water and energy is known as water-energy nexus [9]. The increase in water usage results in an increase in wastewater generation and thus water treatment process are demanding. Wastewater can be used as an alternative energy source due to the high content of organic matter for energy generation. Energy generated from wastewater can improve energy security and reduce environmental burdens. A documented study by University of Cape Town (UCT) on behalf of the Water Research Council (WRC) estimated that 10 GWth of energy could be recovered from wastewater streams in Southern Africa. This is equivalent to 7% of Eskom's existing electrical power supply [10].

1.3 Fuel cells

Fuel cells are the promising alternative power carrier that could help to respond to the issues of fossil fuel and environmental impact issues. Fuel cells produce power through converting chemical energy by means of electrochemical reactions. An example of an electrochemical reaction is

hydrogen and oxygen reaction to produce energy while water is formed as a by-product [11, 12]. Two main categories of fuel cell include high-temperature fuel cells and low-temperature fuel cells. Several established low-temperature fuel cells including alkaline fuel cells (AFCs), proton exchange membrane (PEMFCs), direct methanol (DMFCs), and microbial fuel cells (MFCs). High-temperature fuel cells includes molten carbonate fuel cells (MCFCs), phosphoric acid fuel cells (PAFCs) and solid oxide fuel cells (SOFCs) [13].

1.3.1 Microbial fuel cell (MFC) based technology

MFCs are biofuel cells that represent an innovative method of using microorganisms to generate electricity. This device works like any other fuel cell having two electrodes, anode and cathode, that are joined by an electrical wire and separated by membranes such as proton exchange membranes (PEM) or a salt bridge (shown in Fig 1.3). Initially a salt bridge was used for microbial fuel cell development; however various membrane like PEM and CEM (cation membrane) are readily available in the commercial market [14, 15].

In MFCs, electricity generation involves an oxidation process at the anode and a reduction process at cathode. In an anode chamber, the microorganisms produce electrons, protons and carbon dioxide (CO_2) from the oxidation of organic matter. The electrons are transferred to the anode and are subsequently transferred to the cathode via external circuit (and thus producing electrical current). The proton generated are transferred to the cathode through a proton exchange membrane. At the cathode, the proton, electron and oxygen combine to form water [16, 17].

These technologies hold great promise for both wastewater treatment and electricity generation. The technology is capable of harnessing energy stored in wastewater in the form of electricity via the catalytic reaction of microorganisms. The microorganisms catalytic generate an electrons using metabolism substrate for mediating electron transferred to the anode [18].

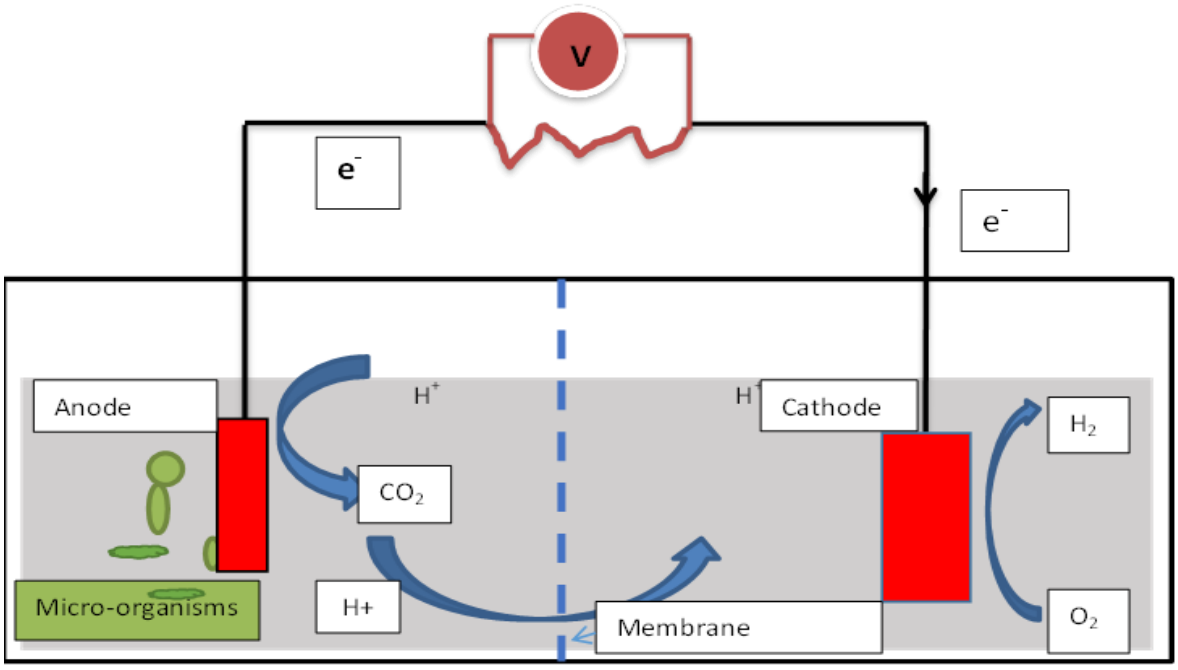

Figure 1.3 Sketch of dual microbial fuel cell (Ahn and Logan, (2010))

1.3.2 Current challenges associated with fuel cells

Low- temperature fuel cells like MFCs used catalysts including enzymes and microbes to reduce oxygen reaction (ORR) to maximise performance. Catalysts are a crucial component of fuel cells and MFC as it determines the efficiency of the system in terms of electricity generation via a redox reaction. In the last few years, many studies have focused on finding some alternative low-cost electro-catalysts such as carbon-based catalysts, manganese oxide, cobalt oxide and iron phthalocyanine to reduce the over potential of the ORR and to replace the conventional costly platinum catalyst for fuel cells. Oxygen reduction reaction (ORR) is describe as a kinetic limitation of electrochemical in MFC and fuel cell in terms of the output. [19, 20]. Platinum and platinum-based material delivers high catalytic performance yet their limited availability and the high cost are serious drawbacks for the development of fuel cells [21].

1.4 Problem statement

The current conventional energy producing techniques rely on fossil fuel that are expensive and have negative environmental impacts. Besides energy producing been expensive consumers feel pressure of high tariffs and interrupted (load shedding) energy supply. The cost of electricity in South Africa has increased over the years. The key challenge is a transition to cleaner sustainable energy supply that is derived from renewable resources. Furthermore, affordable access of this modern sustainable energy services to communities in particular poor rural and urban communities is crucial. MFCs offers an alternative for clean energy generation, with the self-sustaining potential that could alleviate the energy crisis and reduce environmental pollution [22, 23]. There has been immense progress in terms of the design of MFCs such as single or double chamber. Various factors, such as reactor design, type of catalyst, electrode material type and renewable substrate, has increased the possibility of the MFCs technology to be utilised at a commercial scale to produce power and treat wastewater.

Catalysts are a crucial component of MFCs for electricity generation. Platinum and platinum-based material delivers high catalytic performance yet their limited availability and the high cost are serious drawbacks. Significant research is in progress into developing alternative catalysts. Manganese dioxide (MnO_2) is an effective electro-catalyst that have been used for alkaline fuel cells and battery application.

However, there are still many challenges associated with implementing MFCs on a commercial scale. Currently MFCs demonstrates low performance efficiency, expensive materials (catalyst) and activation polarization. This research focus on addressing the effects of introducing a low-cost electro-catalysts material, utilizing wastewater as a fuel source and use a constructed dual chamber MFC system to explore the possibility of generating electricity.

1.5 Research aims and objectives

The focus of this research will be a dual chamber MFC design use wastewater (municipal sewage) and electro-catalyst to generate electricity.

This study can be achieved through the following specific objectives

i. Assess the content of organic matter in municipal (sewage) wastewater in terms of their suitability for power generation using a dual chamber MFC.
ii. Examine the role of manganese oxide (MnO_x) as an electro catalyst for oxygen reduction reaction (ORR) in the MFC while using reduced graphene (rGO) as a support to enhance electrode surface area.
iii. Investigate the effect of graphene material loading on MnO_x catalyst for electrochemistry.

1.6 Dissertation structure

The dissertation consists of six chapters with each chapter concluding with a list of references cited from literature.

1. Chapter 1: General background, aims and the objective of the research including the motivation of this study.
2. Chapter 2: Literature review related to the study is presented.
3. Chapter 3: An experimental method that describes the material and dual chamber design of MFCs, detail information of the synthesis of catalysts, wastewater as a substrate and an anode chamber and electrode modification.
4. Chapter 4: Presents the results and major findings from experimental work.
5. Chapter 5: Discussion of the results.
6. Chapter 6: The conclusions are presented specifically for the set objectives and key questions while the recommendations are presented for future work.

The chapter outlines the focus of the dissertation which is microbial fuel cells (MFCs) based technology. This chapter highlights the environmental, economic and social needs for sustainable renewable energy and outlines the background, problem statement, aims and objectives of the proposed study.

1.7 References

[1] H. Winkler, Renewable energy policy in South Africa: policy options for renewable electricity, Energy Policy, 33 (2005) 27-38.

[2] M.Asif, T.Munee, The status of renewable energy in the GCC countries, Renewable and Sustainable Energy Reviews, 11 (2011) 1388-1413

[3] B.E. Rittmann, Opportunities for renewable bioenergy using microorganisms, Biotechnology and Bioengineering, 100 (2008) 203-212.

[4] A. Pradhan, C. Mbohwa, Development of biofuels in South Africa: Challenges and opportunities, Renewable and Sustainable Energy Reviews, 39 (2014) 1089-1100.

[5] M. Jamil, F. Ahmad, Y.J. Jeon, Renewable energy technologies adopted by the UAE: Prospects and challenges – A comprehensive overview, Renewable and Sustainable Energy Reviews, 55 (2016) 1181-1194.

[6] J. Krupa, S. Burch, A new energy future for South Africa: The political ecology of South African renewable energy, Energy Policy, 39 (2011) 6254-6261.

[7] S. Sgouridis, A. Abdullah, S. Griffiths, D. Saygin, N. Wagner, D. Gielen, H. Reinisch, D. McQueen, RE-mapping the UAE's energy transition: An economy-wide assessment of renewable energy options and their policy implications, Renewable and Sustainable Energy Reviews, 55 (2016) 1166-1180.

[8] A. Pegels, Renewable energy in South Africa: Potentials, barriers and options for support, Energy Policy, 38 (2010) 4945-4954.

[9] Z. Wang, B. Zhang, A.G.L. Borthwick, C. Feng, J. Ni, Utilization of single-chamber microbial fuel cells as renewable power sources for electrochemical degradation of nitrogen-containing organic compounds, Chemical Engineering Journal, 280 (2015) 99-105.

[10] S. Burton, B. Cohen, S. Harrison, S. Pather-Elias, W. Stafford, R. Van Hille, H. Von Blottnitz, Energy from Wastewater-a Feasibility study, WRC, South Africa, (2009).

[11] F. Davis, S.P. Higson, Biofuel cells--recent advances and applications, Biosens. Bioelectron., 22 (2007) 1224-1235.

[12] T. Zhongfu, Z. Chen, L. Pingkuo, B. Reed, Z. Jiayao, Focus on fuel cell systems in China, Renewable and Sustainable Energy Reviews, 47 (2015) 912-923.

[13] R.P. O'Hayre, S.-W. Cha, W. Colella, F.B. Prinz, Fuel cell fundamentals, John Wiley & Sons New York, 2006.
[14] B.E. Logan, Microbial fuel cells, John Wiley & Sons, 2008.
[15] R.M. Allen, H.P. Bennetto, Microbial fuel-cells, Appl. Biochem. Biotechnol., 39 (1993) 27-40.
[16] D.R. Lovley, Microbial fuel cells: novel microbial physiologies and engineering approaches, Curr. Opin. Biotechnol., 17 (2006) 327-332.
[17] H. Liu, B.E. Logan, Electricity generation using an air-cathode single chamber microbial fuel cell in the presence and absence of a proton exchange membrane, Environmental science & technology, 38 (2004) 4040-4046.
[18] R.A. Bullen, T.C. Arnot, J.B. Lakeman, F.C. Walsh, Biofuel cells and their development, Biosens. Bioelectron., 21 (2006) 2015-2045.
[19] M.V. Kannan, G. Gnana kumar, Current status, key challenges and its solutions in the design and development of graphene based ORR catalysts for the microbial fuel cell applications, Biosens. Bioelectron., 77 (2016) 1208-1220.
[20] B.H. Kim, I.S. Chang, G.M. Gadd, Challenges in microbial fuel cell development and operation, Appl. Microbiol. Biotechnol., 76 (2007) 485-494.
[21] M.T. Nguyen, B. Mecheri, A. D'Epifanio, T.P. Sciarria, F. Adani, S. Licoccia, Iron chelates as low-cost and effective electrocatalyst for oxygen reduction reaction in microbial fuel cells, Int. J. Hydrogen Energy, 39 (2014) 6462-6469.
[22] G.D. Najafpour, Chapter 18 - Microbial Fuel Cells: A New Source of Power∗, in: G.D. Najafpour (Ed.) Biochemical Engineering and Biotechnology (Second Edition), Elsevier, Amsterdam, 2015, pp. 527-555.
[23] M. Guo, W. Song, J. Buhain, Bioenergy and biofuels: History, status, and perspective, Renewable and Sustainable Energy Reviews, 42 (2015) 712-725.

CHAPTER 2

2. LITERATURE REVIEW

This chapter presents a review of recent literature regarding microbial fuel cells and their development

2.1 Introduction

Wastewater is usually rich in organic matter and therefore a potential resource for energy, plant fertilizer nutrients and water [18, 24]. In the United States, 0.5-2 kWh/m^3 is required generally for domestic wastewater treatment and consumes approximately 3 to 4% of the U S electrical power which is equivalent to 110 Terawatt hourly per annum [25]. In general, available technologies for wastewater treatment are not sustainable to meet the constantly increasing water sanitation demands due to fast industrialization and population growing. Therefore, there is a need for new technologies that are more efficient and sustainable.

Numerous efforts have been made in eliminating excess sludge and finding a cost effective conventional wastewater technology for clean electrical power and high value products by direct conversion of waste [26]. Domestic wastewater has utilized in biofuel technologies as a source to generate electricity, chemicals and other fuels. In the current market biogas technology is used to harvest energy in a form of methane from wastewater sludge through anaerobic digestion (AD). In addition, energy can be recovered from wastewater sludge using other thermochemical technologies such as gasification, liquefaction and pyrolysis. Furthermore, water reuse has already been widely practiced, especially in some dry areas, but it invariably requires more energy for treatment, principally arising from the increased water quality requirements for reuse.

Technically, an MFC is type of fuel cell. A fuel cell is a form of technology that produces electricity through electrochemical processes instead of combustion. Fuel cells are divided into two groups, namely conventional chemical and biological-based fuel cells. Recently, biological fuel cells such as microbial fuel cells (MFCs) has become an attractive power generation

technology and is being extensively researched. MFC technology has demonstrated the link between the growing field of biotechnology and fuel cells [27]. MFCs work operate in a similar manner to chemical fuel cells, as there is transformation of the organic substrate present in wastewater into electrical energy through electrochemical reactions catalyzed by microbial activity [14, 28]. Recently there have been extensive literature reviews that relate to wastewater being a potential fuel to produce power utilizing MFC technology [29]. On the other hand, traditionally fuel cell produce hydrogen with constant supplier of such as oxygen.

MFCs results in the anaerobic oxidation of organic matter due to microbial activity at the anode while the oxidant is reduced at the cathode. The electron from the anode flows to the cathode through an external circuit to produce electricity. Protons permeate across a membrane and are reduced in the presence of oxygen to produce water [30]. This technology offers a great potential to produce bio-electrochemical energy from wastewater and concurrently remove organic pollutants by means of microorganisms. MFCs can have more advantageous than current biofuel technologies in terms of power generation, economic revenue and environmental sustainability. MFCs benefits power generation, low carbon foot print and water reclamation. MFC also function efficiently at ambient temperatures.

Currently, an improved understanding of electron transfer mechanisms and operating conditions of MFC has led to major improvements in power output. The key challenge in utilizing MFCs is to overcome cathodic reaction or over potential, ohmic losses, high material cost and low power output. MFCs' system performance can be enhanced by the incorporation of a membrane electrode assembly (MEA). The use of an MEA for MFCs may result in a compact design of MFC chambers by minimizing the space between electrodes, which may enhance the current output and decrease internal resistance of the system [31]. Additionally, the cathodic reaction can be overcome with less costly catalyst. To reduce cathode catalyst cost, the following alternative may be utilized: a non-platinum metal, manganese oxide, chemically coated carbon materials, or a composite catalyst [32-34].

2.2 Initial work on MFCs

2.2.1 History

Scientist Luigi Galvani discovered the concept of bioelectricity as early as 1780. His work on frog tissues demonstrated the existence of "animal electricity" [35]. In 1839, Sir William R. Grove, invented the fuel cell system. His study showed a reversal action on electrolysis of water, where the reaction between hydrogen and oxygen produced water and an electric current [36]. M.C Potter, who investigated and demonstrated the generation of electrical power from *Escherichia coli* and *Saccharomyces*, first demonstrated the concept of utilizing microorganisms as a biocatalyst to generate electricity in 1911 [18, 28]. In 1931, Cohen at Cambridge revitalized Potter's works and showed how MFC devices in batch mode generates greater than 35 Volts (V) [37].

Through the US National Aeronautics and Space Administration (NASA), MFCs received increased attention in the 1960s for producing power from organic waste intended for long haul space flights. Later, in the 1970s during the oil crisis interest in MFCs development was revived after it had been discovered that the addition of electron mediators has a great impact in enhancing the current density and the power output [14, 38]. Bennetto and his co-workers introduced the modern design of MFC and the concept how it works in the 1980s [39, 40]. MFCs have come a long way until the early 90s. In the late 1999s wastewater as a substrate played a vital role in enhancing power generation. Before these studies, a chemical mediator was required for MFCs to transport electrons from the bacterial cells to the electrode. These mediator chemicals were often expensive and toxic, therefore creating difficulty in commercialization of MFCs. Kim and his co-workers during (1999s) developed a mediator-ess MFC by discovering that electrons can be transferred outside the cells of certain microbes thus enhancing the commercial viability of MFCs [41, 42]. In 1997, Hasvold established that the bacteria at the cathode act as a catalyst for oxygen reduction.

2.2.2 Basic principles of MFC operation

MFCs are essentially electrochemical power sources that work like galvanic cells. Generally, an MFC comprises of anodic and cathodic electrode physically separated by a proton exchange membrane (PEM). Wastewater containing organic matter is fed to the anode chamber, which is an anaerobic oxidation chamber. Microbes grows on the anode surface as a biofilm and is oxidised which leads to the exergonic formation of electrons and protons. The electrons flow externally of the cell from the anode to the cathode thus creating a current in the circuit. The electrons are reduced at the cathode [43].

The Gibbs energy is an integral measure of an electrochemical reaction. The Gibbs energy of reaction is determined from thermodynamics and is used to calculate the maximum amount of useful work available from the reaction. The standard Gibbs energy can be used to determine a standard cell voltage (or electromotive force, emf). The theoretical cell voltage or electromotive force (emf) is the potential difference between the anode and cathode and represents the systems capability potential for electricity generation.

$$emf(\Delta E^0) = \frac{\Delta G}{nF}$$

$$\Delta E_{cell}{}^0 = \Delta E_{cathode}{}^0 - \Delta E_{anode}$$

where

emf (ΔE^0) = electromotive force (in V)

ΔG = Gibbs energy of the reaction (in J/mol)

n = the number of electrons involved in the reaction (in mol)

F= Faraday's constant (96485.3 C/mol).

The Gibbs energy of the reaction is negative for MFCs. That means, the emf will be positive, representing the potential current generated from the reaction. Acetate has been used as organic

substrate and the following typical redox reaction occurs in an MFC resulting in electricity generation [44]. Equation 1 and 2 below illustrates the redox reactions of MFC diagram using acetate (also Fig 2.1)

Anode: $CH_3COO^- + 4\ H_2O \rightarrow 2HCO_3^- + 9H^+ + 8e^-$ (E^o = -0.289 V *vs.* SHE)

Cathode: $2\ O_2 + 8H^+ + 8e^- \rightarrow 4H_2O$ (E^o = 0.805 V *vs.* SHE)

Total: $CH_3COO^- + 2O_2 \rightarrow 2\ HCO^{3-} + H^+ + H2O$ (ΔG = -847.60 kJ/mol; emf = 1.094 V)

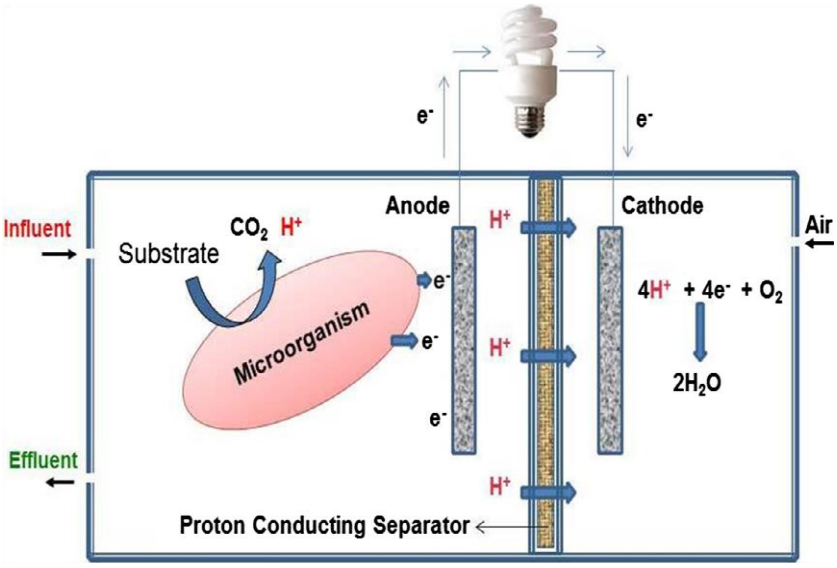

Figure 2.4 H-MFCs type Double Chamber schematic [8].

2.3 Design configuration, electrode material and component

There has been immense progress in terms of the design of MFCs. Various factors, such as reactor design, type of biocatalyst, electrode material type and renewable substrate, has increased the

possibility of the MFCs technology to be utilised at a commercial scale to produce power and treat wastewater.

The recent MFC designs are classified into two groups: laboratory prototypes and commercial prototypes. Laboratory prototypes focus on increasing system efficiency by changing variable parameters (pH, concentration etc.) during test work. Commercial prototypes have a wider application in areas like landfill bioreactor cells, biosensors and wastewater treatment. Numerous laboratory prototypes have been developed for MFCs. However, single and double-chamber designs are the most common. Other prototypes include up-flow and stacked cells with or without a membrane. MFCs technology was considered far from commercialization a few years ago. Recently commercial prototype MFCs have emerged on the market. Companies such as EcoVolt from Cambrian Innovation has developed an MFC based wastewater treatment system. Additionally, companies such as Emefcy and Pilus Energy are about to launch commercial systems [45].

2.3.1 Dual- compartment MFCs design

A dual-compartment MFC operates in either batch mode or continuous mode to produce energy. A cost effective H-shaped dual chamber MFC design is ideal for laboratory-scale and this design was mainly were utilised in the early stages of MFCs research [30].

The anodic component of the MFC releases electrons through an oxidation reaction while reduction reaction takes place at the cathode component (see Fig 2.2 below). Electrons released by microbes at the anode are transported to the cathode through potential gradient (E_{cell}) in between the membrane (PEM/Nafion117). This membrane enables electrons to pass between the anodic and cathodic compartment, making a complete electric circuit. The PEM restricts oxygen diffusion at the anode and permits H^+ ions to flow over to the cathode chamber for reduction.

The commercialisation of the dual-compartment MFC system, as compared to the single-compartment MFC system, has been challenging due to cathode design. In a two-compartment

MFC, the cathode section contains a liquid oxidant such as ferricyanide ($K_3(CN)_6$) that is utilised as a final electron acceptor [46].

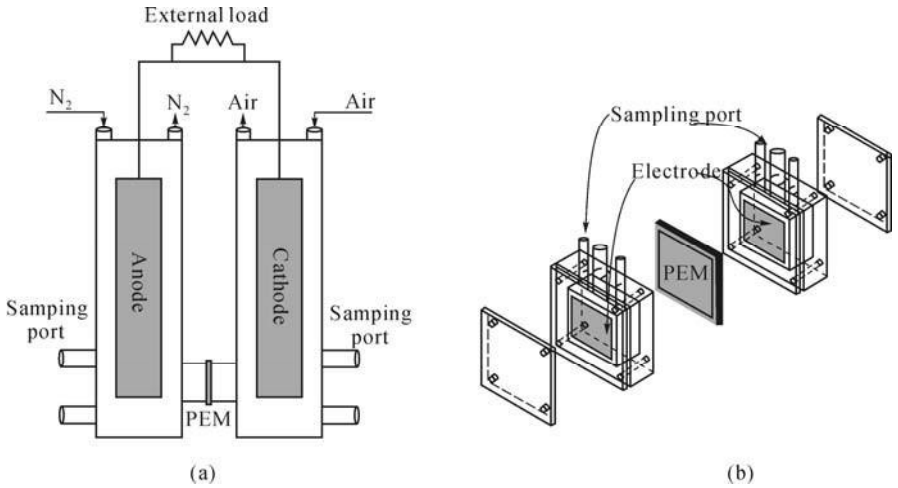

Figure 2.5 Schematic of a two-chambered MFC in cylindrical shape (a) and rectangular shape (b) [26]

2.3.2 Single- compartment MFCs design

The single compartment MFC design has several advantages over the dual-compartment MFC cell such as its simple design and economical operation method. It can operate without aeration and the cathode is directly exposed to air, which decreases the internal ohmic resistance [47]. In some designs in cylindrical shape, a single-compartment MFC consist an anode containing graphite granules (Granular Activated Carbon (GAC)) in a tubular anode compartment, with cathode on the outside that is visible directly to the air [48]. Numerous different types of tubular MFCs have been studied. Studies on a different design of tubular MFCs with the anode and cathode positioned at the upper and lowest of the vertical cylinder respectively both require aerated cathodes and used a glass wool and glass bead filling to separate the anode and cathode compartments. This permit diffusion of protons from the anode to the cathode compartment but limiting the diffusion of air to the anode, permitting it to remain anaerobic. Most single compartment MFCs utilise a membrane-electrode-assemble (MEA) design, whereby the membrane is between the cathode and the anode in a sandwich shape. Most MEA configurations are extensively studied in conventional chemical

fuel cells. However, an MEA incorporated in MFCs can improve current output and columbic efficiency [49, 50].

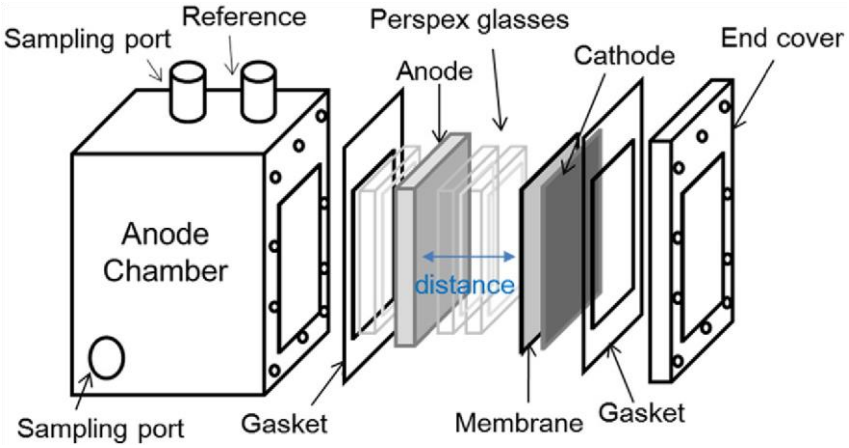

Figure 2.6 Diagram of a single-cube chamber air cathode MFC with an MEA assembly, and representation of the distance between anode and cathode.

2.3.3 Stacked MFCs

A number of MFC compartments can be stacked together in either series or parallel to increase the power generation within the system. Earlier configurations consisted of 12-compartment cell split into 6 dual compartment flat-plate cells with series and parallel connected was used by Aelterman [51]. However, the operation characteristics of the stacked MFC must be steady condition to avoid cell reversal. If the cell is in reversal conditions, MFC with a low catalytic activity will switch polarity and cannot sustain long operation of the systems. Different stacked MFCs compartment has been reported in literature where 0.13mW/cm^2 maximum power densities on an open circuit voltage of 2.5V were obtained. A parallel stack connection gives a high short circuit current when

compare to a series stack connection, suggest that MFCs connected in parallel offers a high bioelectrochemical reaction rate than series connected [52].

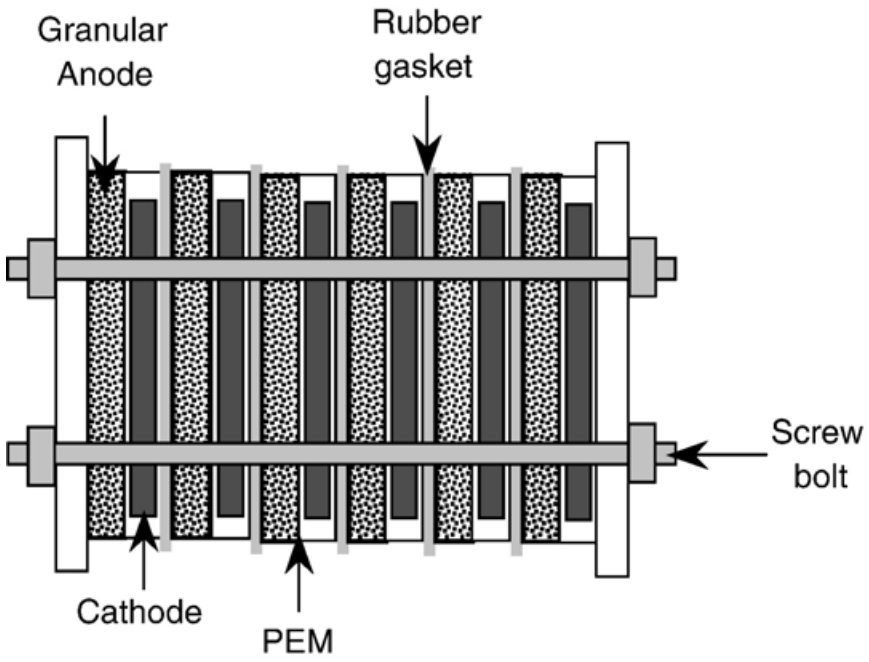

Figure 2.7 Schematic of a Stacked MFC [33]

2.3.4 Up-flow MFC

An Up-flow MFC is more attractive for wastewater treatment because it is easy to scale up and operate in a continuous mode [53]. The Plexiglas cylinder-shaped MFC incorporates an anode at the bottom of the tube and the cathode at the top with glass beads and glass wool located in between the two compartments. For example a substrate (such as biomass /wastewater) diffusion between the electrodes offers a dissolved oxygen gradient which is good for MFC operation [54].

In addition, in this MFC configuration the anode and cathode are close enough above the membrane (PEM) surface area, which gives low internal resistance of 4 Ω [55].

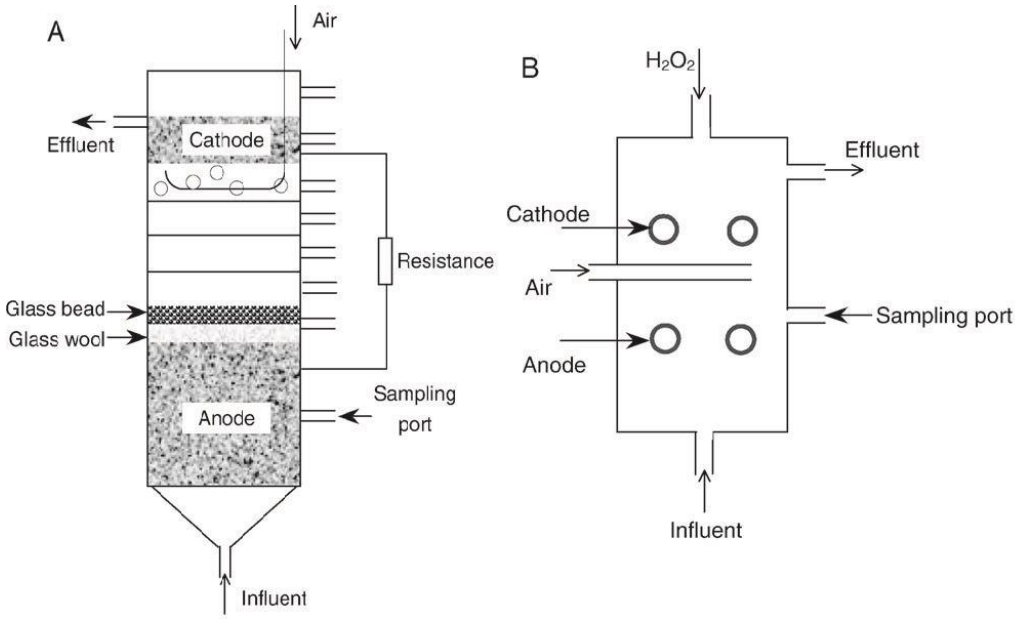

Figure 2.8 Schematics of mediator-and membrane-less MFC with cylindrical shape (A), and with rectangular shape (B) [35]

2.4 Electrode material

Researchers have become more innovative in selecting cost effective construction materials and elements for MFCs systems in order to enhance power generation and scale up MFCs. The power output from MFC technology is linked to the performance of the components of the MFC such as the anode material, buffer solution, cathode material, electrode surface, electrode spacing, configuration, and substrate concentration [56].

The selection of the electrode material is a key parameter influencing power output. The design of a cost effective electrode is a great challenge for the commercial application of MFCs. In addition, electrode materials and should be chemically stable to produce more current and should also be biocompatible, have good mechanical strength and a high conductivity. The maximum surface area of the electrode is another significant aspect for upscaling and also determines the energy output of the system [18].

Currently, carbon in various forms such as graphite plates, rods, felt, cloth and paper are utilised for anode and cathode construction as shown in Fig 2.6. Carbon electrodes are cost effective and easy to handle with a well-defined surface area. On the other hand, platinum (Pt.) and Pt. black electrodes offer a better performance with increased power generation when compared with carbon material.

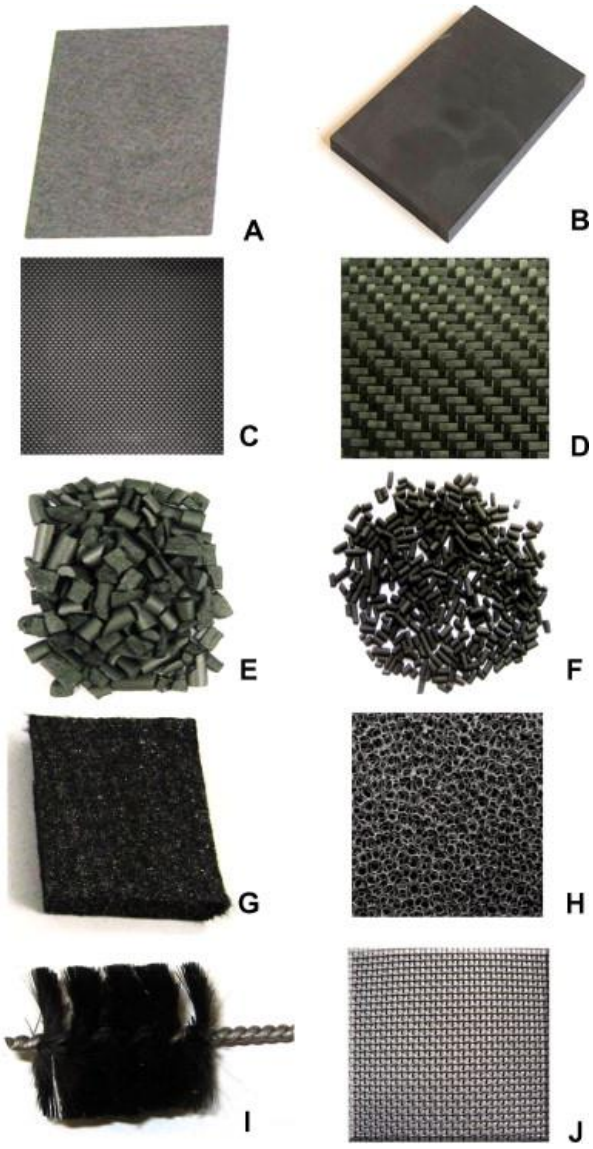

Figure 2.9 Electrode materials used for MFC: (A) carbon paper; (B) graphite plate; (C) carbon cloth; (D) carbon mesh; (E) granular graphite; (F) granular activated carbon; (G) carbon felt; (H) reticulated vitrified carbon; (I) carbon brush; (J) stainless steel mesh

2.4.1 Anode electrode

The modification of an anode electrode, using chemical treatment of non-metallic material or metal coatings reduces the cost and improves MFC performance [57]. The anode material is crucial in terms of high specific surface area, high conductivity, porosity, and limited propensity to fouling or corrosion requirements.

The stability, high electric conductivity and large surface area of carbon based materials including carbon cloth, carbon granules and graphite felt make the most versatile and commonly used anode material in microbial cultures.

2.4.2 Cathode electrode

The electrons and protons produced by fuel oxidation from the anode side travel to the cathode side via an external circuit and membrane respectively. The cathode electrode have great influences on numerous factors, which includes concentration, catalyst electrode modification, proton availability and type of the electron acceptor employed. The most widely used terminal electron acceptor (TEA) is oxygen at the cathode although it requires a high activation energy for the cathode reaction. Ferricyanide (K_3 (CN) $_6$) is a common chemical widely used in lab scale MFCs as an experimental electron acceptor. Ferricynanide has a low resistance as compared to oxygen and effective mass transfer overcomes the activation energy limitation for oxygen reduction at the cathode. However, ferricyanide can diffuse through the membrane into anode space and interfere with bacterial cell.

Cathode electrode must have a high redox potential and able to capture protons. The electrode cost fabrication and its operation in MFC is a big challenge. To overcome challenges related to the cathode, progress has been made on inexpensive cathode catalysts. Alternative noble metal catalysts for cathode such as cobalt-tetramethoxy-phenyl-porphyrin(CoTMPP) iron phthalocyanine (FePc), manganese oxide (MnOx), non-Pt catalyst and carbon based material, which reduce cathodic reaction and deliver good performance results have been investigated .These nanomaterial composites enhances the electrochemical catalytic activity and have a higher surface area than carbon materials coated with platinum [32, 33].

2.4.3 Electro-catalysis in MFC

Currently, researchers are attempting to find a better way of dealing with the oxygen reduction reaction (ORR) in both fuel cells and MFC applications. Oxygen reduction reaction (ORR) is a significant limiting factor in the power generation of MFC technology and also limits the performance of MFCs. Platinum (Pt) has been widely used as a catalyst for the oxygen reduction reaction although it is not cost effective. The high cost and sensitivity to poisons makes Pt catalysts impractical [58]. There is a growing interest in alternative catalysts, which are cost effective and efficient. Various base metals including, cobalt; manganese, iron, copper and nickel have been tested as catalysts to improve the kinetics of ORR and enhance the performance of the MFC [59].

2.4.4 Manganese dioxide (MnO_x) as an alternative electro-catalyst

Manganese dioxide (MnO_2) is an effective electro-catalyst that has been commonly used for alkaline fuel cells and battery application [59]. Manganese oxide (MnO_2) is a high quality electrode material available at a low cost, is environmentally friendly, has a high energy density and is naturally available. MnO_2 has a high conductivity and high structural porosity for ion and gas transport [60]. In addition, MnO_2 has a favourable crystal morphology which makes it particularly useful for improving the kinetics of the oxygen reduction reaction for air electrodes [58]. The ORR mechanism in alkaline media using a MnO_2 catalyst follows a gives partial 2-electron process to reduce O_2 to H_2O; followed by a 2- electron reduction of HO_{2-} to O2 and OH^- (see Fig 2.7). Also the outstanding electro-catalytic activity towards. The resulting four-electron ($4e^-$) reduction of O_2 makes MnO_x is good candidate electrocatalyst.

$$O_2 + 4H^+ + 4e^- \rightarrow 2H_2O \qquad E^0 = 1{:}23V \text{ vs:SHE}$$

$$O_2 + 2H^+ + 2e^- \rightarrow H_2O_2 \qquad E^0 = 0{:}70V \text{ vs:SHE}$$

$$H_2O_2 + 2H^+ + 2e^- \rightarrow H_2O \qquad E^0 = 1{:}78V \text{ vs:SHE}$$

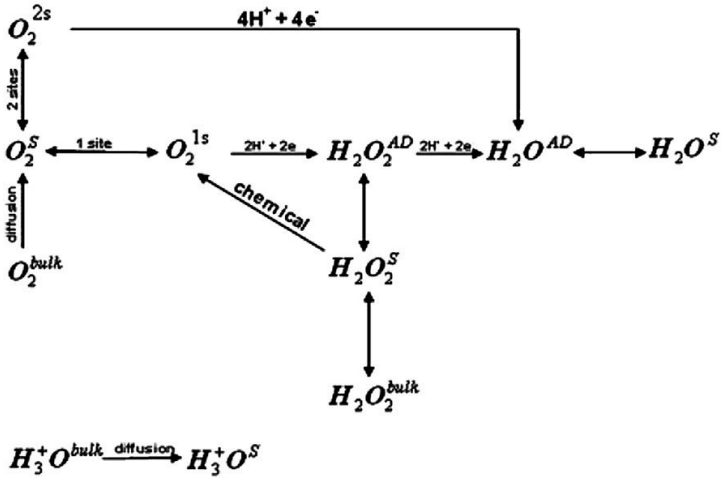

Figure 2.10 The reduction of oxygen showing the 4 e- reduction pathway as well as alternative 1 e-, 2e-, and 3e- reduction pathways [42].

Although progressive research has been conducted in alkaline solution for the electrochemical properties of manganese oxides, more studies on their catalytic activity in neutral solution are required. The ORR chemistry on the surface of the MnO_2 composite is able to prevent the production of peroxide and assist in its decomposition in alkaline and neutral solutions. Manganese oxide structures yield good ORR catalytic activity [61, 62].

2.4.5 Membrane and Separator material

2.4.5.1 Membrane-Proton exchange membrane (Nafion117)

The membrane is at the forefront of MFC design and has cost implications on the process performance. It is important to select a suitable membrane considering oxygen diffusion, substrate loss and internal resistance. Proton electrode membranes (PEM) have been widely utilised in MFCs. DuPont™ Nafion117 membranes (perfluorinated inonom) is commonly used as a proton exchange membranes to separate the anode and cathode chambers [17]. High proton conductivity of PEMs enables proton transfer from the anode to cathode and water leakage is prevented because of its hydrophobic layer. Other cation species such as Na^+, K^+, NH^{4+} or Mg^{2+} are permitted through the Nafion^{TM} 117 membrane at the same speed of H^+. However, PEM contributes to the high price

of MFC systems and reduces the power output through internal resistances. The surface area of the PEM is an important parameter affected the power output, an increase in area results in an increase power density. For example, an MFC producing up to 45 mW/·m^2 of 3.5 cm^2, 68 mW·/m^2 at 6.2 cm^2, and 190 mW·/m^2 at 30.6 cm^2 has been reported [63, 64].

2.4.5.2 Membrane electrode assembly

Membrane electrode assembly (MEA) design in MFC system is a key component of the MFCs system performance. The MEA should have a long lifetime, a high power output and be cost effective to be commercially viable. Although numerous membranes have been tested in chemical fuel cells, more work needs to be done on membranes as applied in MFCs [49, 65].

2.5 Substrate utilized in MFCs

Organic substrates are crucial in MFC operations as the power generation depends on the substrate conversion rate. The efficiency and economic viability of converting organic wastes to bioenergy depended on the characteristics, concentrations and components of the waste material. The organic substrates decomposes to produce electrons the MFCs harvest to produce power. A great variety of substrates can be used in MFCs for electricity production ranging from pure compounds to complex. Various substrate are currently used for MFCs and these are categorized as either natural or synthetic. The use of pure substrates has been ideal for researchers focusing on different fundamental aspects in MFCs operation mainly. The growth medium with pure substrate (carbon sources) and other micronutrients is usually referred to as synthetic wastewater. The organic matter present in wastewater substrates can provide a rough estimate for predicting the power output of complex wastewater substrates [66, 67].

2.5.1 Wastewater substrate

Wastewater is a valuable feedstock for MFCs systems as it contains organic matter that can be used to generate power. Various wastewater have been tested in MFCs and it has been showed that less sludge is produced as compared to biogas processes. Ongoing work is been conducted on wastewaters containing high organic matter as a fuel. Examples of wastewater includes brewery waste, chemical industrial waste, corn stover, and food industry waste, landfill leachates, in palm oil mill effluent areas, in starch processing waste, swine and sanitary wastes [66].

Industrial wastewater can vary tremendously in terms of chemical oxygen demand (COD). Depending on some industrials wastewater are pre-treatment before it can discharged wastewater to municipal treatment plants. However, industrial wastewater can have high concentrations of toxics waste and other value products. MFCs use various bacteria which are efficient in moderating the toxic chemicals and reagents existing in wastewater. For example, the chemical oxygen demand(COD) of wastewater produced from the Fischer-Tropsch (FT) process can be as a high as 30 g/l and contains alcohols, hydrocarbons and monocarboxilic organic acids. MFC can be a suitable technology for the treatment of this kind of industrial wastewater and will decrease the carbon footprint. However, there is no prior research on MFCs technology investigating FT wastewater [24, 68, 69].

The use of landfill leachate as a substrate for MFCs benefits both industrial waste and the environment by mitigating greenhouse gas emissions. Leachate is defined as liquid drawn from waste which contains dissolved or suspended contaminants. MFCs can be utilised to treat landfill leachate without extra substrate, chemicals or inoculation while producing power. This technology can be a feasible choice for leachate treatment and the elimination of major components. The leachate is characterised by a high ammonia concentration, as well as biological oxygen demand(BOD), chemical oxygen demand and total phosphorous [70].

Municipal sewage sludge contains nutrients of value to crops, specifically, nitrogen, phosphorus, potassium, and sulphur. Sewage sludge is produced from municipal wastewater treatment as by-products and is created through sedimentation from primary and secondary treatment. The

treatment and disposal of sewage sludge in municipal wastewater treatment plants is operationally costly. The cost is due to the high organic contents; approximately 66% of the energy content is from primary sludge in wastewater and about 81% of biodegradable organic. This means MFC can harvest energy from municipality sewage sludge [71, 72].

2.6 Characterization of MFCs performance evaluation

The optimization and energy generated in MFCs is dependent on electrochemical reactions. The reactions occurs between organic substrate in anode chamber and the electron acceptor in cathode chamber.

2.6.1 Voltage

Voltage is the key parameter in measuring MFC performance. An ideal MFC performance depends on produce power under constant voltage. The power depends on both voltage (V) and current (I). The relationship of this variable is dictated by the fuel cell resistance, which is known as Ohm's law

$$V = I \times R$$

V =the voltage (V),
I = the current density (A cm^2)
R= represents the resistance (Ohm).

The voltage output between MFC and chemical fuel cells are differ since the condition of microorganisms in the anode is unpredictable. Mixed culture (with different microorganisms) are commonly used in the anode chamber [30].

2.6.2 Power generation

The power output of an electrochemical process is very important aspect of MFC performance. The amount of energy is determined by following equation.

$$P = V \times I$$

Where P represent power (Watts).

The potential in MFCs reactor is constantly measured and current is determined by:

$$E = P \times \mathrm{t}$$

where E (V) is the cell potential,
(P) the power (Watts)
(t) time (s).

2.6.3 Coulombic efficiency

The consumption of organic compounds determines the Coulombic efficiency for power power generation. The Coulombic efficiency (εC), is defined as the ratio of total Coulombs actually transferred to the anode from the substrate (C_p) to the maximum possible Coulombs (C_n) if all the substrate is being removed to produce power;

$$\varepsilon \mathrm{C} = \frac{\mathrm{C}\rho}{\mathrm{C}n} \times 100\%$$

$\mathrm{C}p$ is determines by integrating the current over time and $\mathrm{C}n$ is calculated as follows

$$CE = \frac{M \int_o^{tb} Idt}{\Delta COD F n v_{MFC}}$$

where, CE is the columbic efficiency, F is Faradays constant (96458 ^oC/mol of electrons)
where M is molecular weight of oxygen (32 g/mol), n=4 is number of electrons exchanged per mole of oxygen, t_b is operating time of the experiment, V_{MFC} is volume of the dual chambered MFC (m^3) and ΔCOD is the difference in COD between influent and effluent.

2.6.4 Polarization curves

A polarization curve depicts against current. In many cases, the output of an MFC is analyzed using this tool. Polarization curves represents the change in the voltage by varying an external resistance. The current can be obtained by dividing the voltage with the external resistance applied. The power curve displays how the power varies as the current changes (Fig 2.8). The highest point in the power curve specifies the maximum power and the external resistance is equivalent to the internal resistance during open circuit voltage (OCV) measurement.

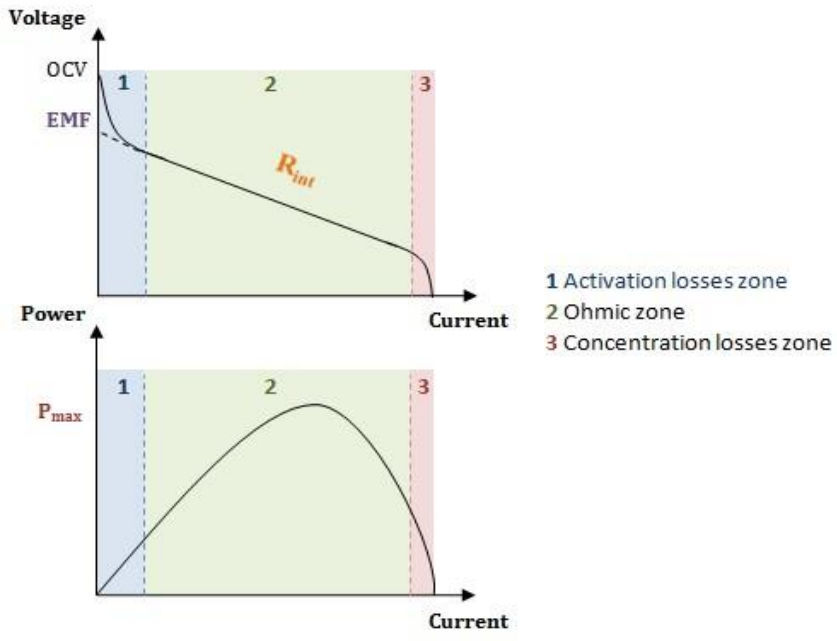

Figure 2.11 A polarization curve and (1) a power curve [56].

The polarization curve represents the decrease in voltage in three regions. The first region shows a low current area under a high external resistance conditions with the voltage dropping rapidly and the current flows via a circuit as an indication of activation losses. The second region indicates concentration loss at high current with a fast drop in voltage under a low external resistance and the third region is an intermediate current with a consistence voltage decrease indicating external resistance loses due to Ohmic losses.

An activation loss causes energy loss during an electron transfer from the cell terminal to the anode surface during the oxidation and reduction reaction. The insufficient flux of reactants to the electrode causes losses in concentration and mass transfer limitations. This generally occurs when the rate of reaction is fast at a high current. Ohmic losses are caused by a resistance to the flow of ion in the solution and the membrane and the resistance of the transfer of electrons through the electrodes. Ohmic losses can be eliminated in different ways, including electrode spacing minimization or using a membrane with higher proton conductivity and increasing electrode solution conductivity.

2.7 Other wastewater treatment and Power generation

2.7.2 Bioremediation

Recently, MFC technology has been applied to the bioremediation of wastewater as well as rivers, lakes and the coastline. Bio-remediates for wastewater including various organic pollutants (such as hydrocarbons) and inorganic streams such as ammonia waste streams and nitrates [56].

2.7.2 Bio-hydrogen

Microbial electrolysis cells (MECs) produces hydrogen through a biological process. Microbial electrolysis cells are able to generate hydrogen at the cathode electrode with an additional voltage in the circuit while oxidizing organic matter at the anode. The development of MECs are identical to MFCs with a similar reactor design and anode reaction. In the hydrogen economy, microbial electrolysis cells could potentially offer hydrogen as a renewable source [73].

2.7.3 Bio-sensing

Biosensor also known as biological sensor, the device is employed with a transducer (which converts one form of energy to another) and a biological element such as a microorganism. Biochemical oxygen demand (BOD) is generally used to evaluate the content of organic matter in wastewater. Those organic substances are converted into electricity using MFCs through microbial catabolism, works as a transducer in microbial biosensors. Certain microbial fuel cells-based biosensor has been extensively utilised to measure biochemical oxygen demand (BOD) and water toxicity. There is a linear relationship between the coulombic yield of microbial fuel cells and BOD. The microbial fuel cells sensor provides a good relationship between the BOD value and the coulombs generated and have functioned for over 5 years and have been stable without any monitoring. The high sensitivity and selective sensing capability of microbial fuel cells are generally used in various fields ranging from environmental monitoring, food and fermentation industry and clinical diagnostic [74, 75].

2.8 References

[1] V.G. Gude, Wastewater Treatment in Microbial Fuel Cells – An Overview, Journal of Cleaner Production.

[2] R.A. Bullen, T.C. Arnot, J.B. Lakeman, F.C. Walsh, Biofuel cells and their development, Biosensors and Bioelectronics, 21 (2006) 2015-2045.

[3] P.L. McCarty, J. Bae, J. Kim, Domestic Wastewater Treatment as a Net Energy Producer–Can This be Achieved?, Environmental Science & Technology, 45 (2011) 7100-7106.

[4] P. Manara, A. Zabaniotou, Towards sewage sludge based biofuels via thermochemical conversion – A review, Renewable and Sustainable Energy Reviews, 16 (2012) 2566-2582.

[5] B.S. Singu, K.R. Yoon, Porous manganese oxide nanospheres for pseudocapacitor applications, Journal of Alloys and Compounds, 695 (2017) 771-778.

[6] R. Allen, H.P. Bennetto, Microbial fuel-cells, Applied Biochemistry and Biotechnology, 39-40 (1993) 27-40.

[7] B.E. Logan, Microbial fuel cells, John Wiley & Sons, 2008.

[8] P. Pandey, V.N. Shinde, R.L. Deopurkar, S.P. Kale, S.A. Patil, D. Pant, Recent advances in the use of different substrates in microbial fuel cells toward wastewater treatment and simultaneous energy recovery, Applied Energy, 168 (2016) 706-723.

[9] B.E. Logan, B. Hamelers, R. Rozendal, U. Schröder, J. Keller, S. Freguia, P. Aelterman, W. Verstraete, K. Rabaey, Microbial Fuel Cells: Methodology and Technology†, Environmental Science & Technology, 40 (2006) 5181-5192.

[10] S. Hays, F. Zhang, B.E. Logan, Performance of two different types of anodes in membrane electrode assembly microbial fuel cells for power generation from domestic wastewater, Journal of Power Sources, 196 (2011) 8293-8300.

[11] R. Burkitt, T.R. Whiffen, E.H. Yu, Iron phthalocyanine and MnOx composite catalysts for microbial fuel cell applications, Applied Catalysis B: Environmental, 181 (2016) 279-288.

[12] F. Zhao, F. Harnisch, U. Schröder, F. Scholz, P. Bogdanoff, I. Herrmann, Application of pyrolysed iron(II) phthalocyanine and CoTMPP based oxygen reduction catalysts as cathode materials in microbial fuel cells, Electrochemistry Communications, 7 (2005) 1405-1410.

[13] K.B. Liew, W.R. Wan Daud, M. Ghasemi, K.S. Loh, M. Ismail, S.S. Lim, J.X. Leong, Manganese oxide/functionalised carbon nanotubes nanocomposite as catalyst for oxygen

reduction reaction in microbial fuel cell, International Journal of Hydrogen Energy, 40 (2015) 11625-11632.
[14] M. Piccolino, Animal electricity and the birth of electrophysiology: the legacy of Luigi Galvani, Brain Research Bulletin, 46 (1998) 381-407.
[15] A.J. Appleby, From Sir William Grove to today: fuel cells and the future, Journal of Power Sources, 29 (1990) 3-11.
[16] U. Schröder, J. Nießen, F. Scholz, A generation of microbial fuel cells with current outputs boosted by more than one order of magnitude, Angewandte Chemie International Edition, 42 (2003) 2880-2883.
[17] I. Karube, T. Matsunaga, S. Mitsuda, S. Suzuki, Microbial electrode BOD sensors, Biotechnology and Bioengineering, 19 (1977) 1535-1547.
[18] H.P. Bennetto, G.M. Delaney, J.R. Mason, S.D. Roller, J.L. Stirling, C.F. Thurston, The sucrose fuel cell: Efficient biomass conversion using a microbial catalyst, Biotechnol Lett, 7 (1985) 699-704.
[19] G.M. Delaney, H.P. Bennetto, J.R. Mason, S.D. Roller, J.L. Stirling, C.F. Thurston, Electron-transfer coupling in microbial fuel cells. 2. performance of fuel cells containing selected microorganism—mediator—substrate combinations, Journal of Chemical Technology and Biotechnology. Biotechnology, 34 (1984) 13-27.
[20] J.B.A. Arends, J. Desloover, S. Puig, W. Verstraete, Principles and Technology of Microbial Fuel Cells, in: Fuel Cell Science and Engineering: Materials, Processes, Systems and Technology, Wiley-VCH Verlag GmbH & Co. KGaA, 2012, pp. 147-184.
[21] B.H. Kim, D.H. Park, P.K. Shin, I.S. Chang, H.J. Kim, Mediator-less biofuel cell, in, Google Patents, 1999.
[22] D.A. Lowy, L.M. Tender, J.G. Zeikus, D.H. Park, D.R. Lovley, Harvesting energy from the marine sediment–water interface II: Kinetic activity of anode materials, Biosensors and Bioelectronics, 21 (2006) 2058-2063.
[23] R.A. Rozendal, H.V.M. Hamelers, K. Rabaey, J. Keller, C.J.N. Buisman, Towards practical implementation of bioelectrochemical wastewater treatment, Trends in Biotechnology, 26 (2008) 450-459.
[24] V.G. Gude, Wastewater treatment in microbial fuel cells – an overview, Journal of Cleaner Production, 122 (2016) 287-307.

[25] K. Rabaey, W. Verstraete, Microbial fuel cells: novel biotechnology for energy generation, Trends in Biotechnology, 23 (2005) 291-298.
[26] D.K. Daniel, B. Das Mankidy, K. Ambarish, R. Manogari, Construction and operation of a microbial fuel cell for electricity generation from wastewater, International Journal of Hydrogen Energy, 34 (2009) 7555-7560.
[27] D. Park, J. Zeikus, Impact of electrode composition on electricity generation in a single-compartment fuel cell using Shewanella putrefaciens, Appl Microbiol Biotechnol, 59 (2002) 58-61.
[28] J. Jiang, Q. Zhao, J. Zhang, G. Zhang, D.-J. Lee, Electricity generation from bio-treatment of sewage sludge with microbial fuel cell, Bioresource Technology, 100 (2009) 5808-5812.
[29] L. Wang, S.G. Advani, A.K. Prasad, Membrane Electrode Assembly with Enhanced Membrane/Electrode Interface for Proton Exchange Membrane Fuel Cells, The Journal of Physical Chemistry C, 117 (2013) 945-948.
[30] P. Clauwaert, D. van der Ha, N. Boon, K. Verbeken, M. Verhaege, K. Rabaey, W. Verstraete, Open Air Biocathode Enables Effective Electricity Generation with Microbial Fuel Cells, Environmental Science & Technology, 41 (2007) 7564-7569.
[31] P. Aelterman, K. Rabaey, H.T. Pham, N. Boon, W. Verstraete, Continuous Electricity Generation at High Voltages and Currents Using Stacked Microbial Fuel Cells, Environmental Science & Technology, 40 (2006) 3388-3394.
[32] I. Ieropoulos, J. Greenman, C. Melhuish, Microbial fuel cells based on carbon veil electrodes: stack configuration and scalability, International Journal of Energy Research, 32 (2008) 1228-1240.
[33] Z. Du, H. Li, T. Gu, A state of the art review on microbial fuel cells: A promising technology for wastewater treatment and bioenergy, Biotechnology Advances, 25 (2007) 464-482.
[34] J.K. Jang, T.H. Pham, I.S. Chang, K.H. Kang, H. Moon, K.S. Cho, B.H. Kim, Construction and operation of a novel mediator- and membrane-less microbial fuel cell, Process Biochemistry, 39 (2004) 1007-1012.
[35] B. Tartakovsky, S.R. Guiot, A Comparison of Air and Hydrogen Peroxide Oxygenated Microbial Fuel Cell Reactors, Biotechnology Progress, 22 (2006) 241-246.
[36] H. Moon, I.S. Chang, B.H. Kim, Continuous electricity production from artificial wastewater using a mediator-less microbial fuel cell, Bioresource Technology, 97 (2006) 621-627.

[37] D.H. Park, J.G. Zeikus, Improved fuel cell and electrode designs for producing electricity from microbial degradation, Biotechnology and bioengineering, 81 (2003) 348-355.
[38] K. Watanabe, Recent Developments in Microbial Fuel Cell Technologies for Sustainable Bioenergy, Journal of Bioscience and Bioengineering, 106 (2008) 528-536.
[39] X. Li, B. Hu, S. Suib, Y. Lei, B. Li, Manganese dioxide as a new cathode catalyst in microbial fuel cells, Journal of Power Sources, 195 (2010) 2586-2591.
[40] W.J. Basirun, M. Sookhakian, S. Baradaran, Z. Endut, M.R. Mahmoudian, M. Ebadi, R. Yousefi, H. Ghadimi, S. Ahmed, Graphene oxide electrocatalyst on MnO_2 air cathode as an efficient electron pump for enhanced oxygen reduction in alkaline solution, Scientific Reports, 5 (2015) 9108.
[41] X.-W. Liu, X.-F. Sun, Y.-X. Huang, G.-P. Sheng, K. Zhou, R.J. Zeng, F. Dong, S.-G. Wang, A.-W. Xu, Z.-H. Tong, H.-Q. Yu, Nano-structured manganese oxide as a cathodic catalyst for enhanced oxygen reduction in a microbial fuel cell fed with a synthetic wastewater, Water Research, 44 (2010) 5298-5305.
[42] A.A. Mirghni, M.J. Madito, T.M. Masikhwa, K.O. Oyedotun, A. Bello, N. Manyala, Hydrothermal synthesis of manganese phosphate/graphene foam composite for electrochemical supercapacitor applications, Journal of Colloid and Interface Science, 494 (2017) 325-337.
[43] S. Chen, J. Zhu, X. Wu, Q. Han, X. Wang, Graphene Oxide−MnO_2 Nanocomposites for Supercapacitors, ACS Nano, 4 (2010) 2822-2830.
[44] C. Zhang, P. Liang, X. Yang, Y. Jiang, Y. Bian, C. Chen, X. Zhang, X. Huang, Binder-free graphene and manganese oxide coated carbon felt anode for high-performance microbial fuel cell, Biosensors and Bioelectronics, 81 (2016) 32-38.
[45] H. Liu, B.E. Logan, Electricity generation using an air-cathode single chamber microbial fuel cell in the presence and absence of a proton exchange membrane, Environmental science & technology, 38 (2004) 4040-4046.
[46] S.-E. Oh, B. Logan, Proton exchange membrane and electrode surface areas as factors that affect power generation in microbial fuel cells, Appl Microbiol Biotechnol, 70 (2006) 162-169.
[47] M.G. Buonomenna, J. Bae, Membrane processes and renewable energies, Renewable and Sustainable Energy Reviews, 43 (2015) 1343-1398.

[48] J.M. Moon, S. Kondaveeti, T.H. Lee, Y.C. Song, B. Min, Minimum interspatial electrode spacing to optimize air-cathode microbial fuel cell operation with a membrane electrode assembly, Bioelectrochemistry, 106, Part B (2015) 263-267.
[49] L. He, P. Du, Y. Chen, H. Lu, X. Cheng, B. Chang, Z. Wang, Advances in microbial fuel cells for wastewater treatment, Renewable and Sustainable Energy Reviews.
[50] D. Pant, G. Van Bogaert, L. Diels, K. Vanbroekhoven, A review of the substrates used in microbial fuel cells (MFCs) for sustainable energy production, Bioresource Technology, 101 (2010) 1533-1543.
[51] B. Min, J. Kim, S. Oh, J.M. Regan, B.E. Logan, Electricity generation from swine wastewater using microbial fuel cells, Water Research, 39 (2005) 4961-4968.
[52] F.J. Hernández-Fernández, A. Pérez de los Ríos, M.J. Salar-García, V.M. Ortiz-Martínez, L.J. Lozano-Blanco, C. Godínez, F. Tomás-Alonso, J. Quesada-Medina, Recent progress and perspectives in microbial fuel cells for bioenergy generation and wastewater treatment, Fuel Processing Technology, 138 (2015) 284-297.
[53] W.-W. Li, H.-Q. Yu, Z. He, Towards sustainable wastewater treatment by using microbial fuel cells-centered technologies, Energy & Environmental Science, 7 (2014) 911-924.
[54] B. Min, B.E. Logan, Continuous electricity generation from domestic wastewater and organic substrates in a flat plate microbial fuel cell, Environmental science & technology, 38 (2004) 5809-5814.
[55] S.T. Oh, J.R. Kim, G.C. Premier, T.H. Lee, C. Kim, W.T. Sloan, Sustainable wastewater treatment: How might microbial fuel cells contribute, Biotechnology Advances, 28 (2010) 871-881.
[56] B.E. Logan, J.M. Regan, Microbial fuel cells-challenges and applications, Environmental science & technology, 40 (2006) 5172-5180.
[57] I. Karube, T. Matsunaga, S. Suzuki, A new microbial electrode for BOD estimation, Journal of Solid-Phase Biochemistry, 2 (1977) 97-104.
[58] B. Kim, I. Chang, G. Cheol Gil, H. Park, H. Kim, Novel BOD (biological oxygen demand) sensor using mediator-less microbial fuel cell, Biotechnol Lett, 25 (2003) 541-545.

CHAPTER 3.

3. EXPERIMENTAL METHODS

3.1 Introduction

This chapter gives a detailed description of the experimental techniques adopted and work procedure in this study. The microwave assisted–hydrothermal techniques is regarded as most viable and cost-effective for synthesize electro-catalysts synthesis of manganese dioxide (MnO_2). Modified Hummer's method will be also used for graphene oxide (rGO) preparation. The synthesis MnO_2-GO will be tested in dual chamber MFC for power generation. The details of a two-compartment MFC design and cell components are provided. The experimental setup and method used are then outlined and lastly the details of various diagnostics tests performed are presented. The material used to construct the MFC structure was Plexi-glass.

The equipment used in this study was accessible at the University (UNISA, Florida Campus) Chemical engineering laboratories and Physics laboratories.

3.2 Experimental procedure

Ultra-pure water (Milli-Q) was used throughout the course of this study to prepare all reagents and for rinsing of all glassware. The chemical reagents used in the experimental work were all analytical grade. Major chemical reagents and material are listed in Table 3.1.

Table 3.1 Chemical and material list

Chemical reagent	Supplier	other information
Potassium permanganate-($KMnO_4$)	Sigma- Aldrich	Analytical grade
Ethanol	Sigma- Aldrich	Analytical grade
Manganese sulfate- ($MnSO_4.H_2O$)	Sigma- Aldrich	Analytical grade
Graphite flake	Merck	Analytical grade
Nafion 117	Sigma- Aldrich	Analytical grade
Nitric acid	Sigma- Aldrich	Analytical grade
Wastewater (Daspoort treatment works)	Collected	
Copper wire	0.5mm diameter, high purity: 99.99%	
Metratlit 2^+Universal TRMS- digital multi-meter	Gossen Metrawatt-Germany	

3.3 Synthesis of Manganese Dioxides (MnO_2)

Microwave assisted–hydrothermal techniques will be used to synthesize manganese dioxide catalyst. Graphene oxide (rGO) will be deposited on the MnO_2 catalyst surface for MFC cathode electrode to improve the oxygen reduction reaction and enhanced MFC power output.

3.4 Microwave-assisted -Hydrothermal method (M-H method)

Microwave assisted-hydrothermal (M-H) synthesis is advantageous over other developed techniques such as sol gel synthesis, sonochemical synthesis, hydrothermal synthesis and microwave-assisted techniques for preparing MnO_2, as it significantly reduces synthesis time, temperature and pressure. This technique uses the advantages of hydrothermal and microwave-assisted synthesis to prevent aggregating of synthesized materials. Heating using microwave irradiation occurs via two mechanisms, (1) dipole polarization and ionic conduction, (2) interfacial polarization that enhances crystallization kinetics of the synthesis process, produces a narrow size distribution of particles with high purity, greater homogeneity of material, higher

yield and control morphology of inorganic materials. The M–H method is energy-saving and economical [76].

MnO_2 was prepared through microwave assisted-hydrothermal method (M–H) under mild conditions. MnO_2 was prepared by mixing 5.34 g of $KMnO_4$ with 7.65g of $MnSO_4.H_2O$ in 250 ml of deionized water. The mixture was stirred with a magnetic stirrer to obtain a homogeneous solution at room temperature. A 40ml vial solution was transferred to a Teflon (PTFE)-lined microwave reactor. The solution loaded into a microwave oven preheated to 90^oC for 30 min, under a pressure of 90 bar and 700 W power (SynthWAVE Microwave, Milestone). The MnO_2 sample in a single-mode microwave oven was also pre-pressurized with N_2 gas. The reaction system was cooled down to room temperature. A black precipitate is finally collected, washed thoroughly with 80ml Milli-Q ultra-pure water and 30ml absolute ethanol, and dried at 75^oC for 8 h under vacuum.

3.5 Synthesis of Graphene Oxide (rGO)

Graphene oxide **(**rGO) was prepared from graphite powder flakes according to modified Hummer's method [77]. Typically, 0.5 g of graphite powder and 0.5 g of $NaNO_3$ were mixed with 23 mL of concentrated sulphuric acid (H_2SO_4) under magnetic stirring for 10 min in an ice bath. Under vigorous stirring, 3 g of $KMnO_4$ was added slowly to avoid a temperature increase above 20^oC. The dark greenish solution was transferred to a water bath at 35^oC and stirred for 1 h. Thereafter 50 mL of water added and the solution stirred for 30 min at 90^oC. Additional 150 mL of water was added and 3 mL of H_2O_2 (30%) was added slowly, resulting in the formation of a brownish solution. Finally, warm solution filtered and washed with 50 mL of 0.1 M hydrochloric acid (HCl) solution and 500 mL of water (H_2O) respectively. The filter cake was then dispersed in water by sonication using a table-top ultrasonic cleaner.

3.6 Membrane preparation

The Nafion 117 membrane cut into a circle with the diameter of 2cm. The membrane was boiled in 3 % hydrogen peroxide for 1 hour and then rinsed in Milli-Q ultra-pure water. This served to clean the membrane and therefore remove any unwanted impurities. The membrane was then treated in boiling 1M H_2SO_4 for 1hour and rinsed again in boiling water several times to sulphonate the membrane.

3.7 Characterization of MnO2 on graphene oxide(GO) support

Manganese dioxide (MnO_2) is an attractive inorganic material due to its atomic structure and attractive chemical and physical properties. MnO_2 is widely employed in catalysis, ion exchange, molecular adsorption, biosensor, and mostly energy storage [78, 79]. The surface of MnO_2 electro-catalysts demonstrates outstanding bi-functional catalytic activity towards the oxygen evolution reaction (OER) and oxygen reduction reaction (ORR) in alkaline medium. MnO_2 exists in some different crystallographic forms such as α, β, γ, δ and variety of morphologies. MnO_2 properties can be characterized by some various techniques, such as scanning electron microscopy (SEM), thermogravimetric analysis (TGA), Fourier transform infrared spectroscopy (FTIR), Brunauer, Emmett and Teller (BET) surface area and porosity analysis, and powder X-ray diffraction (XRD).

3.7.1 Brunauer-Emmett-Teller (BET) surface area analysis.

BET theory deals with physical adsorption of gas molecules on a solid surface which incorporates multilayer coverage. The technique measures the specific surface area of materials. To measure this surface area, solid samples must be dry through heat, vacuum, and the use of gas flow to remove adsorbed contaminants acquired from atmospheric exposure. The solid sample is cooled down under vacuum, normally to a cryogenic temperature of 77 K (-195^{o}C). The adsorption of nitrogen at 77 K and at sub-atmospheric pressures is commonly used and can be used for routine quality control, as well as for investigation of new materials. After each dose, the pressure is allowed to equilibrate and the quantity adsorbed is calculated [80].

The quantity adsorbed at each pressure (and temperature) defines an adsorption isotherm, from which the quantity of gas required to form a monolayer over the external surface of the solid is determined. With the area covered by each adsorbed gas molecule known, the surface area can be calculated.

The theory of the BET incorporate Langmuir which is the concept of monolayer coverage of the solid surface by the adsorptive [81]. BET equation is expressed in this form.

$$\frac{n}{n_m} = \frac{C\frac{p}{p^o}}{\left(1-\frac{p}{p^o}\right)\left(1-\frac{p}{p^o}+C\frac{p}{p^o}\right)}$$ [81].

P and P^o are the equilibrium and the saturation pressure of the adsorbates at the temperature of adsorption and *C* is a dimensionless constant.

The technique evaluates the external area and the pore to area evaluation to determine the total specific area in m^2/g. This provides important information regarding the effects of surface porosity and particle size in many applications. The BJH analysis (Barrett, Joyner, and Halenda) is also employed to determine pore area and specific pore volume using adsorption and desorption techniques. This technique characterises pore size distribution independent of external area due to particle size of the sample.

BET surface areas were determined using a Micromeritics 3 Flex instrument shown in Fig 3.1. About 0.2 g of a sample was degassed at 250^{o}C for 3 hours under vacuum and after that degas in situ carried on at 350 for 4 hours. After the degassing process the samples were analysed using a fully automated analyser [82].

Figure 3.12 Micromeritics 3 Flex instrument used for BET.

3.7.2 Fourier Transform Infrared Spectroscopy (FTIR)

The chemical structure of the sample is examined through Fourier transform infrared spectroscopy (FTIR) (Fig 3.2). Infrared (IR) radiation passes through a sample and some of the radiation will be absorbed by the sample and some will be transmitted or reflected. The resulting spectrum will represent the molecular absorption and transmission, creating a molecular fingerprint of the sample. This makes FTIR spectroscopy useful for several types of analysis such as identifying unknown materials. The FTIR spectra were obtained using a Vetex 70 Bruker FTIR instrument over the range of 4800-50cm^{-1} with standard KBr beam splitter and a resolution of 4 cm^{-1}. A small amount of material was placed on the diamond coated detector and pressed onto the electrode to get FTIR measurements. The spectral data were collected with OPUS 7 software provided on the Vetex70 machine.

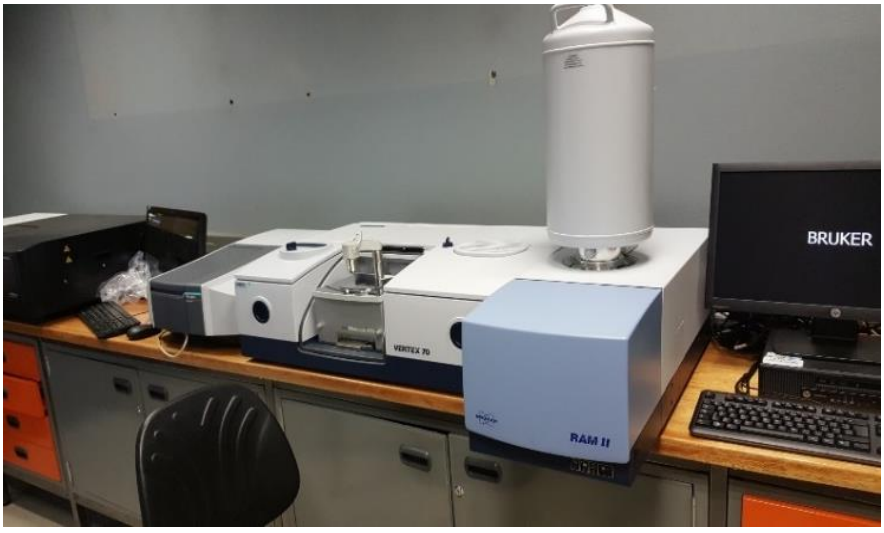

Figure 3.13 Vetex 70 Bruker FTIR instrument.

3.7.3 Thermo-gravimetric analysis (TGA)

TGA is a technique where material weight change as the temperature increases over time in an atmosphere of nitrogen and inert air or other gas. The thermal properties and decomposition temperature of the samples were measured using thermogravimetric analysis (TGA-4000 Perkin Elmer). TGA data was obtained with Pyris software under nitrogen flow. Approximately 10 mg of the sample and the gas flow rate was adjusted to 20 mL/min. The sample was heated from 35^{o}C to 900^{o}C at a heating rate of 10^{o}C/min.

3.7.4 Scanning electron microscopy (SEM)

The SEM uses a focused beam of high-energy electrons systematically to scan across the surface of a specimen. An electron beam is generated using an electron gun. The electron-optical column, through which the beam passes, is operated under high vacuum conditions to allow for a free path for the electrons to pass through and also to avoid high voltage discharge. The beam is accelerated at a high voltage and directed towards the specimen using electromagnetic lenses. The condenser lens is the first lens, which converges the beam and causes the beam to pass through a focal point just above a condenser aperture. The morphology and cross-section of the MnO_2 nanoparticles will be characterized by JSM-6010PLUS/LV-JOEL (see Fig 3.3) operating at 20.0kV. The samples were prepared by placing some of the nanoparticle materials onto an aluminium stub using adhesive carbon tape. The samples were sputter-coated with gold to prevent charging effects inside the microscope. Then the sample was loaded into a chamber using a pin stub mount gripper.

Figure 3.14 JSM-6010PLUS/LV-JOEL scanning electron microscope (SEM).

3.7.5 The powder X-Ray Diffraction

X-ray diffraction (XRD) is a commonly used technique for wide-ranging crystalline material. This technique has been adopted to identify and determine structure phases of material. It is used to determine the average spacing between layers or rows of atoms, and to determine the orientation of a single crystal or grain. X-ray powder diffraction is used to characterise several types of micro and nano-crystalline materials. The complexity crystal structure and the

crystallite size for most applications is where more information extracted based on material nature [83].

The Bragg's law defines the x-ray diffraction sources, where constructive interference of x-rays, condition of scattered from atomic planes of a crystal. The Bragg's law equation 3.1 and schematic interference of radiation between atomic planes in a crystal below Fig3.4.

$$2dsin\theta = n\lambda$$

Where *d* is a interplanar distance for a crystalline solid and the waves are scattered from lattice planes.

θ scattering angle is where the phase shift causes constructive interferences.

λ is the wavelength of the x-ray

n is a positive integer

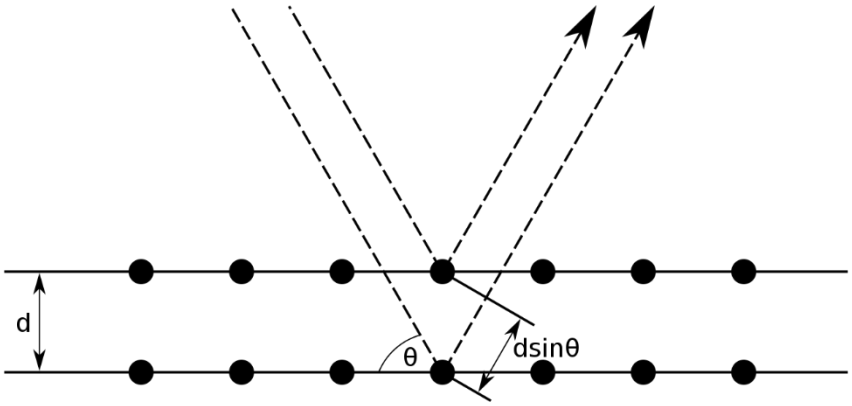

Figure 3.15. Interference of radiation between atomic planes in a crystal [9].

In this study the structural characterization of composite MnO_2 X-ray diffraction (XRD) analysis was investigated by using a SmartLab (Rigaku) diffractometer with Cu Ka radiation (k = 1.5406 Å), employing a scanning rate of $0.2s^{-1}$ and range from 10 to 80. With a beam voltage and a beam current of 30 kV and 15 mA respectively.

3.7.6 Electrochemistry Study

Electrochemical impedance spectroscopy (EIS) is a technique that use small AC amplitude signals to the study the electrical characteristics of an electrochemical cell without affecting its properties. The kinetics of an electrode-electrolyte interface can also be characterised through EIS. The Autolab PGSTAT302N (Metrohm Autolab BV,Netherlands,) utilising NOVA1.10 software was used for EIS analysis of the MnO_2-GO and MEAs with a frequency range of 0.1 to 50,000 Hz. A standard three-electrode system was used for all electrochemical work. The working electrode, platinum as the counter-electrode and Ag/AgCl (3 M KCl) as the reference electrode in 2mM potassium ferricyanide and 2mM KCL electrolyte [84].

3.7.7 Cyclic Voltammetry

Cyclic voltammetry (CV) is a potentiostatic technique and is a commonly used electrochemical technique. In CV, the current response of the working electrode as a function of the applied potential. CV works by scanning the potential of the working electrode linearly from an initial potential to the switching potential, and then the voltage is reversed. In this work, cyclic voltammetry (CV) measurements were done to investigate the electrochemical processes and determine the capabilities of MnO_2-GO catalyst based.

In MFCs, CV is used to determine the electrochemical surface areas of the electrode. The Autolab PGSTAT302N was used for CV analysis which was performed by cycling the potential between 0.02 to 0.8 V at a different scan rate of 10, 20, 30, 40, 50,100 and 200 mV/s. In MFCs, CV is used to determine the electrochemical surface areas of the electrode. The Autolab PGSTAT302N was used for CV analysis which was performed by cycling the potential between 0.02 to 0.8 V at a scan rate of 50 mV/s [85].

3.7.8 Fabrication of working electrode- Glassy Carbon electrode (GCE)

The working electrodes ink was prepared using the following method:

- 9.8 mg of synthesized nanocomposite (MnO_2) mixed with 5 wt% PTFE binder.
- About 4.15ml deionized water and 0.830ml ethanol was added to the mixture to get a homogenous slurry.

- The resultant mixture was then sonicated in an ice bath for 60 min to obtain a uniform suspension.
- The Glassy Carbon electrode (GCE) tip was modified by dropping 10 µl of the ink solution and allowing it to dry overnight. The MnO_2 electrocatalyst loading in this study was maintained at 20µg.cm^{-2}.

The second working electrode MnO_2-GO was prepared by the same procedure. A 4.9mg of synthesized nanocomposite (45 wt % MnO_2) and 4.9mg GO (45 wt % GO) with 20 µl of Nafion117 (5 wt% PTFE binder) manufactured by DuPont. A 4.5ml of water and 0.830ml ethanol was then added to the mixture to get 5ml homogenous solution. The resultant mixture was then sonicated in an ice bath for 60 min to obtain a uniform suspension. The GCE tip was modified by dropping 10 µl of the ink solution and allowing it to dry overnight.

3.8 Method and Experiment Design

3.8.1 MFC set-up

The experiments were carried out in dual compartment MFC from Plexiglas. The compartment with a total volume 2750cm^3 consisted of an anode, proton exchange membrane and cathode. The dimension of the MFC were 0.4cm thickness, height 20cm, length 21cm and width 10.5cm. An external resistance was ranging from 1000 Ω to 1.000 Ω used to complete the circuit. The effective volume both for anode and cathode was 2722 cm^3. There was no oxygen crossover in this assembled cell and the anode can easily be sustained under anaerobic conditions as shown in Fig 3.5.

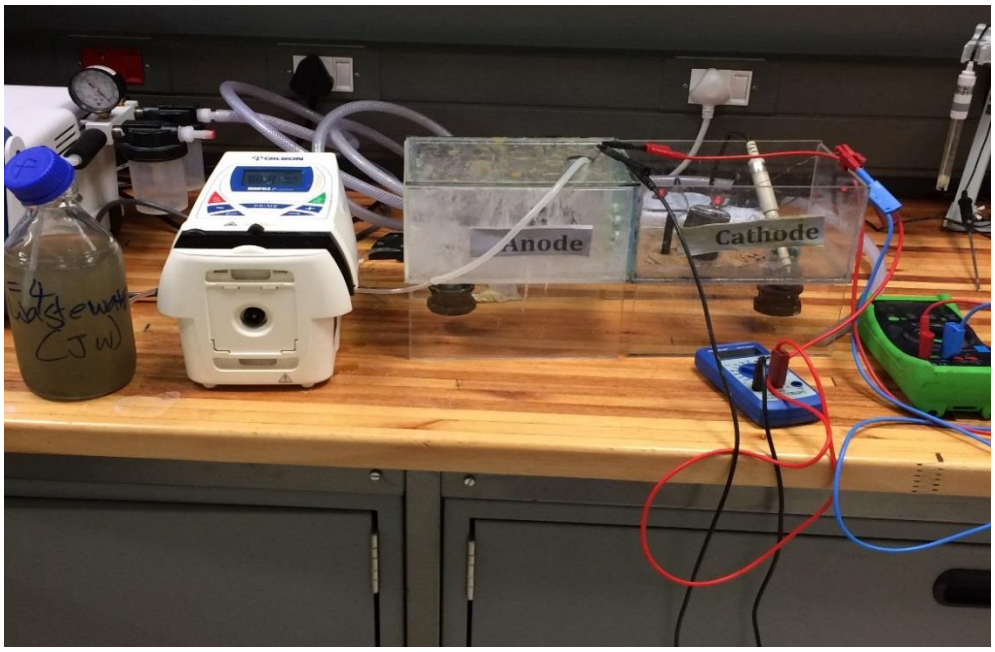

Figure 3.16. Constructed Dual chamber MFC set experimental.

3.8.2 Wastewater Sampling

Municipality sewage wastewater will be sampled by the grab sampling method from the Daspoort wastewater treatment works in Pretoria (South Africa). Prior to feeding the MFCs, the wastewater was stored at 4^{o}C in a refrigerator and adjust to room temperature before being used. The municipality sewage wastewater COD measurements will be performed according to the APHA standard protocol, 1998 and with a spectrophotometer (Spectroquant Nova 30, Merck, Germany) [86]. The pH and conductivity were both measured with a 700 Eutech instrument/pH meter.

3.8.2 MFC operation

MFC will operate in a continuous-fed mode by pumping wastewater directly to the anode compartment at the rate of 70 ml/ min using a peristaltic pump (Gilson's MINIPULS Evolution, Middleton, USA) equipped with Marprene II tubing (Watson-Marlow). On the other hand, the cathode chamber was filled with potassium ferricyanide (50mM $K_3Fe(CN)_6$) the catholyte. The pH ranged from 6.5 to 8.0 maintained at room temperature (25^{o}C). Air (1.5 mbar per min) was percolated in the cathode chamber through a vacuum pump to supply molecular oxygen as an electron acceptor for the cathode.

3.8.3 Electrode-Anode and Cathode

The electrode was designed, constructed and supplied by Electro Carbon in Boksburg, South Africa. The electrode was modified according to size and shape. Information regarding the electrodes is tabled in table 3.2. The cathode electrode was catalysed with MnO_2 with projected surface area of $11cm^2$, thickness of 4.0 mm and total weight of 90.7g and modified size is 4.2g. (Shown in Fig 3.6) The operating temperature of the substrate ranged between 25ºC-40ºC.

Table 3.2 Graphite rod and additional component

Component	quantity	Material	Specification
Graphite rod	4	Carbon material	0.049m
Material type		Component element	Specification
Additional			
Nuts	8	Plastic	
Washer	8		
O-ring	8		

Figure 3.17. Graphite electrode

References

[1] B. Ming, J. Li, F. Kang, G. Pang, Y. Zhang, L. Chen, J. Xu, X. Wang, Microwave–hydrothermal synthesis of birnessite-type MnO_2 nanospheres as supercapacitor electrode materials, Journal of Power Sources, 198 (2012) 428-431.

[2] W.S. Hummers, R.E. Offeman, Preparation of Graphitic Oxide, Journal of the American Chemical Society, 80 (1958) 1339-1339.

[3] J.R. Trapero, L. Horcajada, J.J. Linares, J. Lobato, Is microbial fuel cell technology ready-An economic answer towards industrial commercialization, Applied Energy, 185, Part 1 (2017) 698-707.

[4] A. Fraiwan, S. Choi, A stackable, two-chambered, paper-based microbial fuel cell, Biosensors & Bioelectronics, 83 (2016) 27-32.

[5] K. Sing, The use of nitrogen adsorption for the characterisation of porous materials, Colloids and Surfaces A: Physicochemical and Engineering Aspects, 187–188 (2001) 3-9.

[6] S. Brunauer, P.H. Emmett, E. Teller, Adsorption of Gases in Multimolecular Layers, Journal of the American Chemical Society, 60 (1938) 309-319.

[7] J.C. Groen, L.A.A. Peffer, J. Pérez-Ramírez, Pore size determination in modified micro- and mesoporous materials. Pitfalls and limitations in gas adsorption data analysis, Microporous and Mesoporous Materials, 60 (2003) 1-17.

[8] R. Guinebretière, X-ray diffraction by polycrystalline materials, John Wiley & Sons, 2013.

[9] J. Als-Nielsen, D. McMorrow, Front Matter, in: Elements of Modern X-ray Physics, John Wiley & Sons, Inc., 2011, pp. i-xii.

[10] A.J. Bard, L.R. Faulkner, Electrochemical Methods: Fundamentals and Applications, Wiley, 2000.

[11] N. Aristov, A. Habekost, Cyclic Voltammetry - A Versatile Electrochemical Method Investigating Electron Transfer Processes, World Journal of Chemical Education, 3 (2015) 115-119.

[12] A. American Public Health, A.D. Eaton, A. American Water Works, F. Water Environment, Standard methods for the examination of water and wastewater, APHA-AWWA-WEF, Washington, D.C., 2005.

CHAPTER 4

4. RESULTS AND DISCUSSION

This chapter firstly present catalysts design characterization results and followed by the application on MFC generating electricity.

4.1. Characterizations of manganese dioxide nanoparticles

4.1.1. X-ray Diffraction (XRD) of MnO_2

XRD measurements was carried to investigate the crystal structures and phase of synthesized MnO_2. It is found that the sharp and high intensity peaks correspond to α-MnO_2 and the results are shown in Fig 4.1.

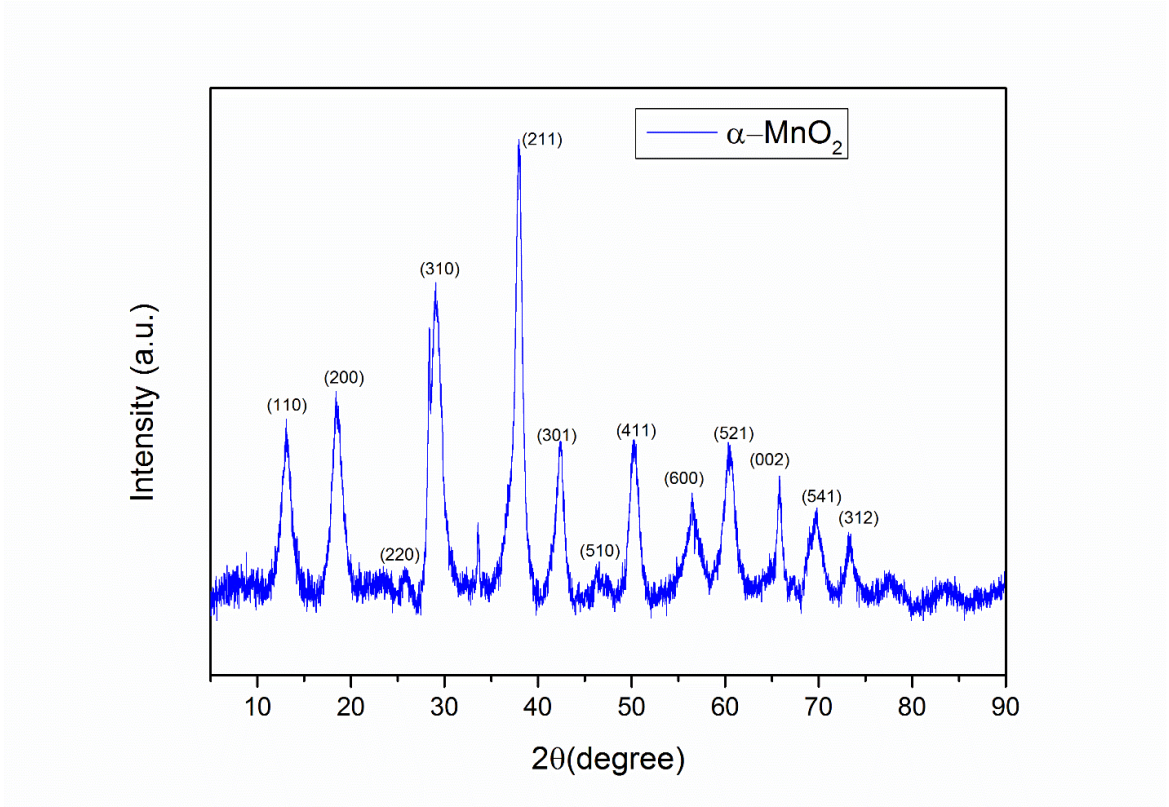

Figure 4.18. X-ray diffraction patterns of α-MnO_2 synthesized microwave –hydrothermal technique

X-Ray diffraction patterns of the α-MnO_2 clearly show the characteristic planes of the tetragonal α-MnO_2 phase at a series of peaks 2θ = 12.72º (110), 18.04º (200), 26.21º (310), 29.21º (310), typical diffraction 2θ = 37.36º (211), 42.23º (301), 46.37^0 (510), 50.08º (411), 56.06º(600), 59.51º(521), 65.10º(002), 69.90º(541) and 73.07º(312). This indicates a high crystallinity and high purity of the α-MnO_2 prepared by the microwave hydrothermal synthesis. The peaks and values are in very good agreement with the literature values (JCPDS 44–0141) [87].

4.1.2. X-ray Diffraction (XRD) of Graphene Oxide (GO)

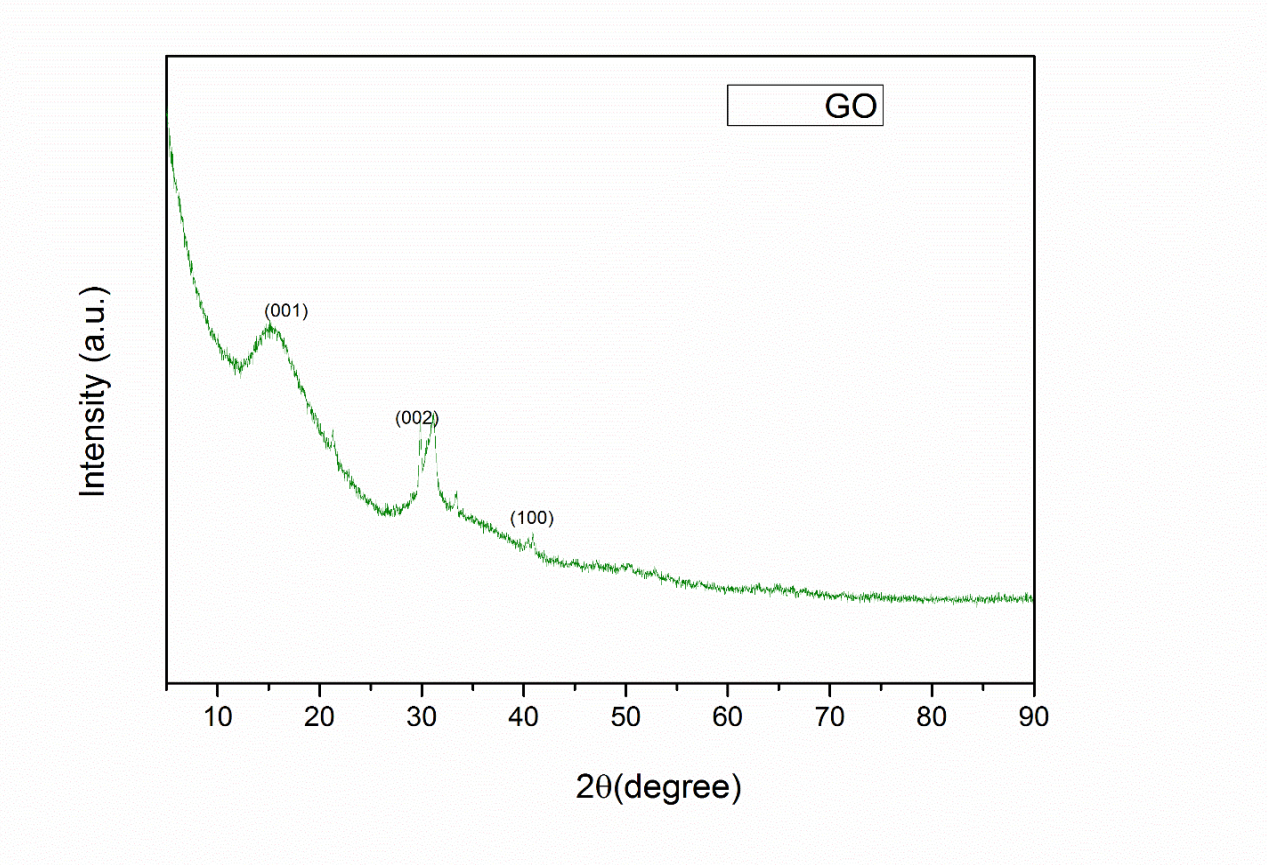

Figure 4.19. X-ray diffraction patterns of GO

The XRD pattern of GO shown in Fig 4.2 reveals peak at 2θ = 11.75° (001) which correspond to the normal diffraction peak of GO powder. The new diffraction peak also traced at 2θ = 24.05º which indicates successful oxidation of graphite to GO. In addition, intense and sharp peak locate at 2θ = 26.85º (002) correspond to high crystallinity of graphite [88] [77]. As for the diffraction pattern, the peaks located at around 43.1° is also associated to the graphite-like (100) reflection.

4.1.3. X-ray diffraction patterns of α-MnO_2-GO

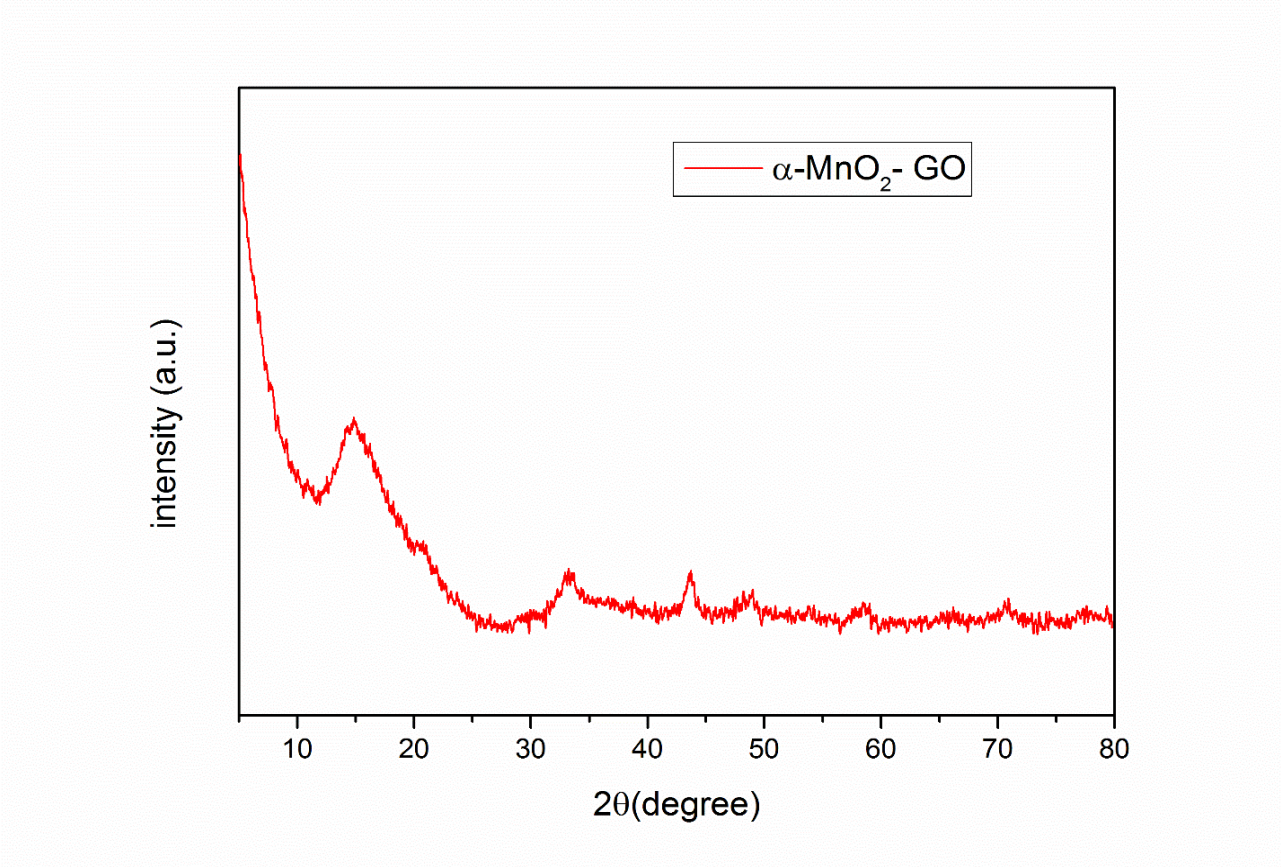

Figure 4.20 X-ray diffraction patterns of α-MnO_2-GO

The peaks in XRD pattern of α-MnO_2-GO composite confirms monoclinic structure of birnessite-type MnO_2 with mixed crystalline and amorphous parts. Intense peaks relate to a poor crystallized originated from the small particle size and around amorphous nature of the powder. Crystal plane of graphene cannot be detected after the deposition of α-MnO_2, indicates that the surfaces of graphene are totally covered by nanoscale α-MnO_2, results in the low degree of graphitization.

4.2. FT-IR spectra of synthesized α-MnO_2 ,GO and α-MnO_2-GO

From the analysis, all the essential characteristic functional groups for α-MnO_2 were identified as showed in Fig 4.4. The peak emerged at 3011 cm^{-1} is signified to the O-H stretching vibrations of water molecules and basis hydroxyl groups, at 1358 cm^{-1} the peak is due to the bending vibration of the O-H groups of the absorbed water. The absorption peak detected at 1733 cm^{-1} resembles C=O groups and 1206 cm^{-1} peak is a stretching vibration absorption. The two absorption peaks located at 476 cm^{-1} and 632 cm^{-1} assigned to Mn-O stretching of the octahedral layers is the birnessite structure [89, 90].

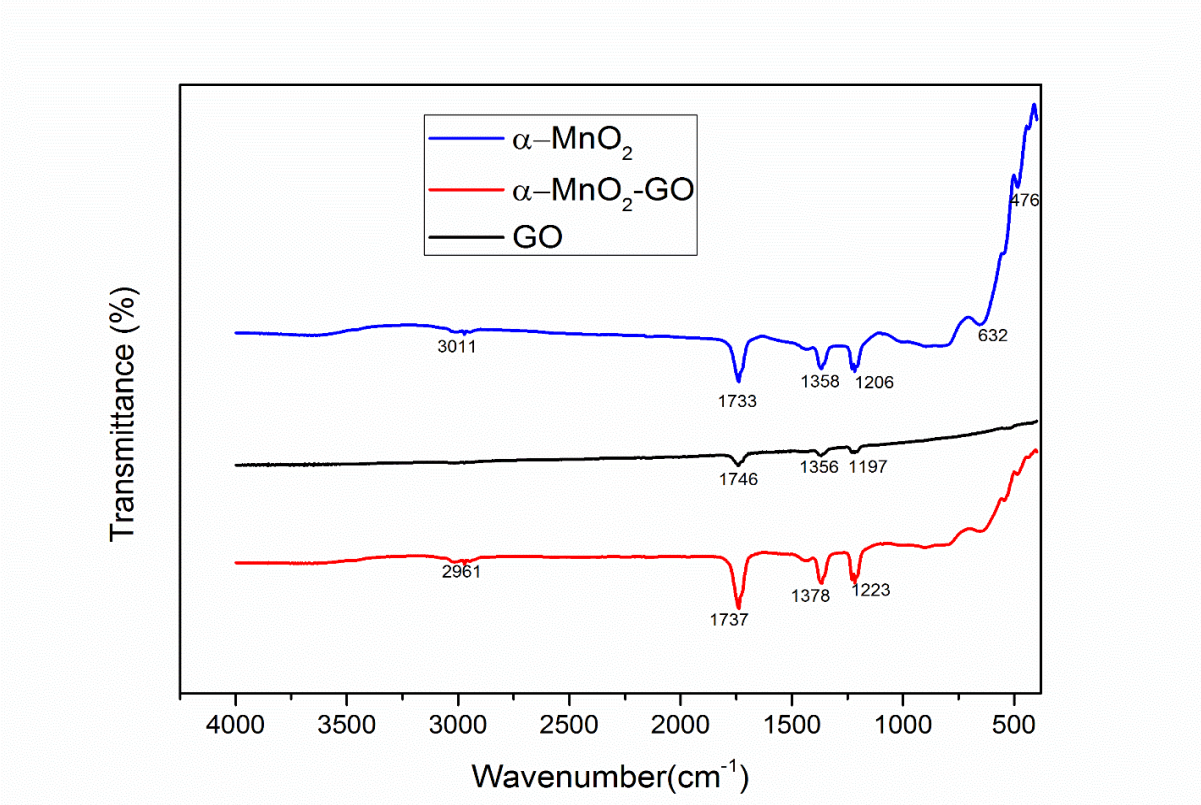

Figure 4.21 FTIR spectra of α -MnO_2 synthesised, GO and α-MnO_2-GO

The FTIR analyses of GO is also illustrated in Fig 4.4. a peak indicated at 1746 cm^{-1} is an absorption band which resemble a stretching vibrations of carbonyl and carboxyl (C=O). The band around 1197 cm^{-1} indicates the presence of C-O (epoxy). Moreover, another peak is at 1356 cm^{-1} can attribute to vibration of C-O (carboxyl).

For composite sample α-MnO_2-GO, the peaks at 1746 cm^{-1},1356 cm^{-1} and 1197 cm^{-1} attributes to O-H, C=O and C-O respectively. In addition, MnO_2 peaks assigned to the Mn-O lattice vibration and Mn-O-Mn vibration corresponding the presence of MnO_2 particles in α-MnO_2-GO [91].

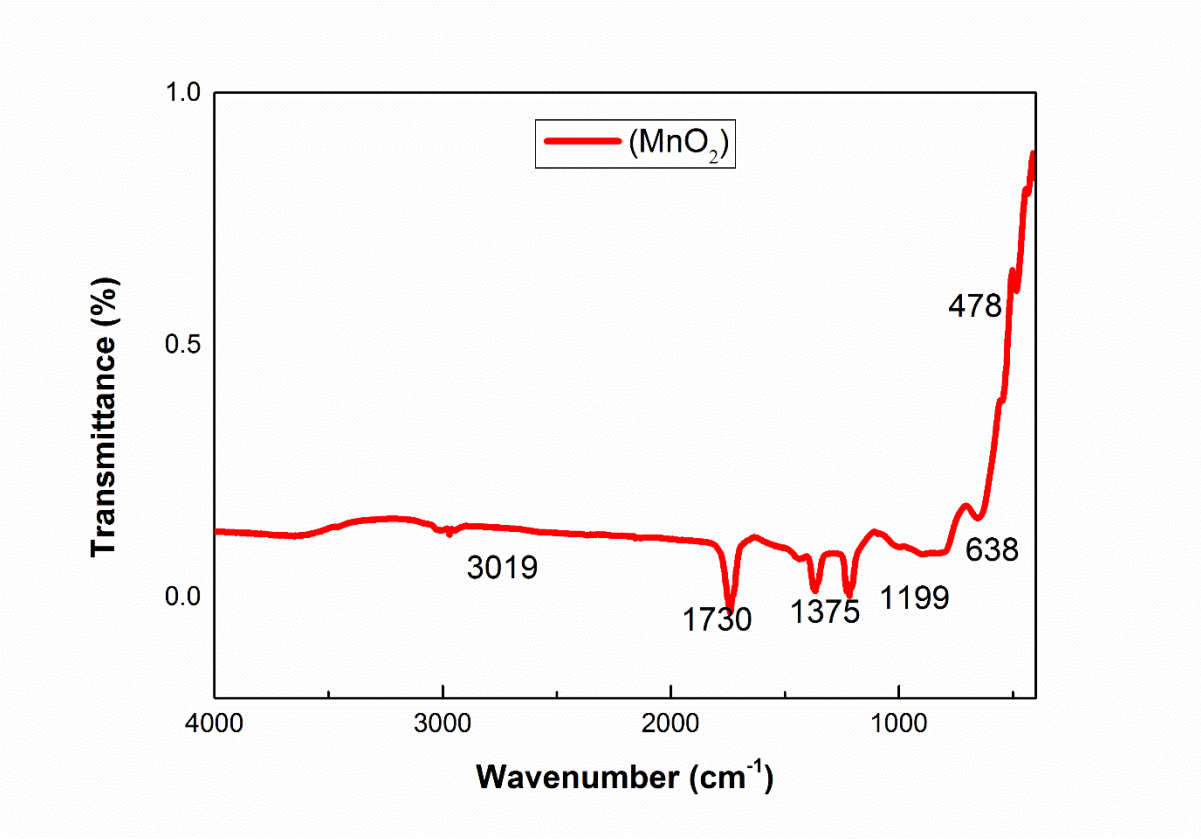

4.3. Thermo-gravimetric (TGA) analysis of α-MnO_2 , GO and MnO_2-GO

The thermogravimetric curve and thermograms of α-MnO_2 are shown in Fig 4.5. A-MnO_2 composite exhibited lightweight loss at the start when temperature increase from 34ºC to 122ºC, which is attributed to the removal of physically adsorbed water. At 100–616ºC temperature, range the weight loss is due to dehydration of crystalline water and electrode surface cracking. At this point 616ºC, α-MnO_2 transformed into crystalline Mn_2O_3 and another weight loss at 887ºC corresponds to phase transition from Mn_2O_3 to Mn_3O_4. The weight loss at this point is due to 20% adsorbed water as compared to 39% hydration of MnO_2 [92].

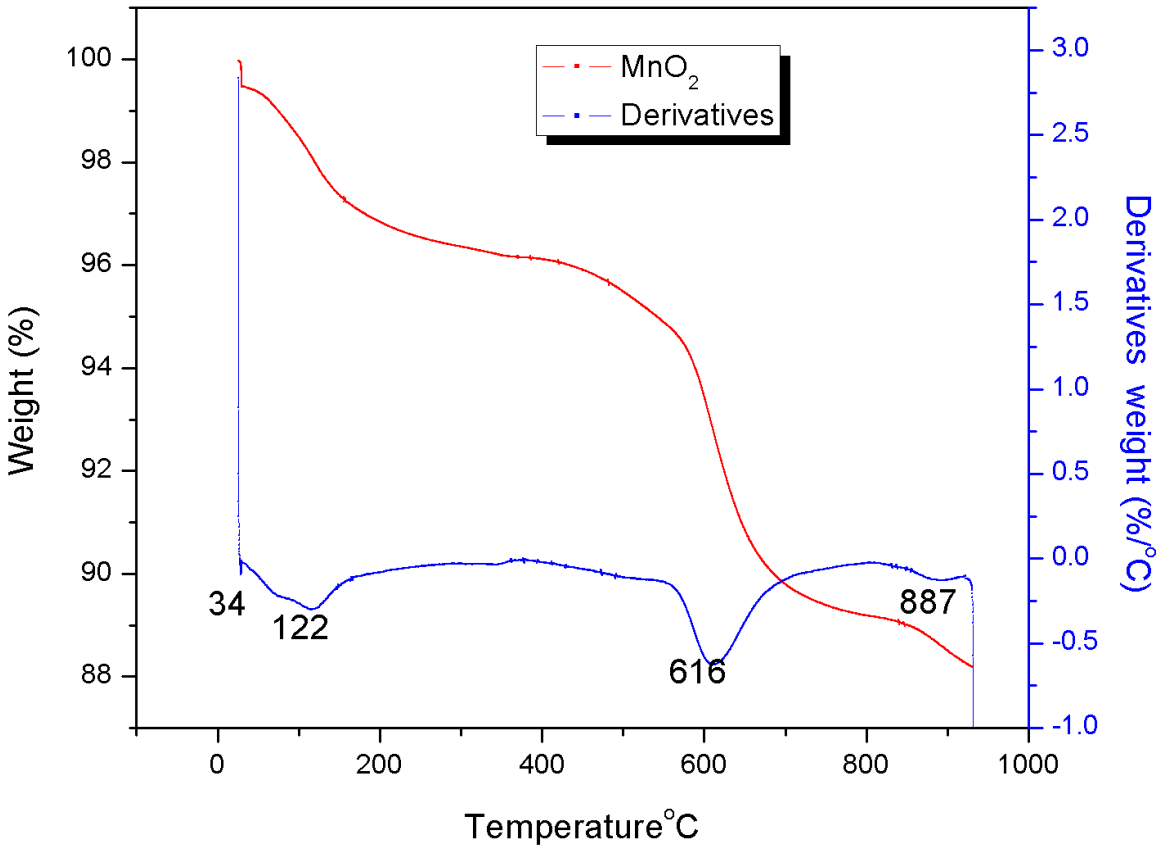

Figure 4.22 TGA curves of the synthesized α-MnO_2 with derivatives weight (% /ºC)

TGA curves of GO material Fig 4.6 showed weight loss from room temperature to 148 ºC due to the absorbed water molecules. After 148 ºC, GO material is fairly stable and the further weight loss can be seen at 555ºC for decarboxylation. Further, weight loss of GO up to 690 ºC and indicating complete decomposition up to 900 ºC. The carboxyl, epoxy, hydroxyl functional groups over GO surface area appears during the oxidations of graphite powder induces by oxygen, which destructed the conjugated sp^2 hybridized network and reduces GO thermal stability.

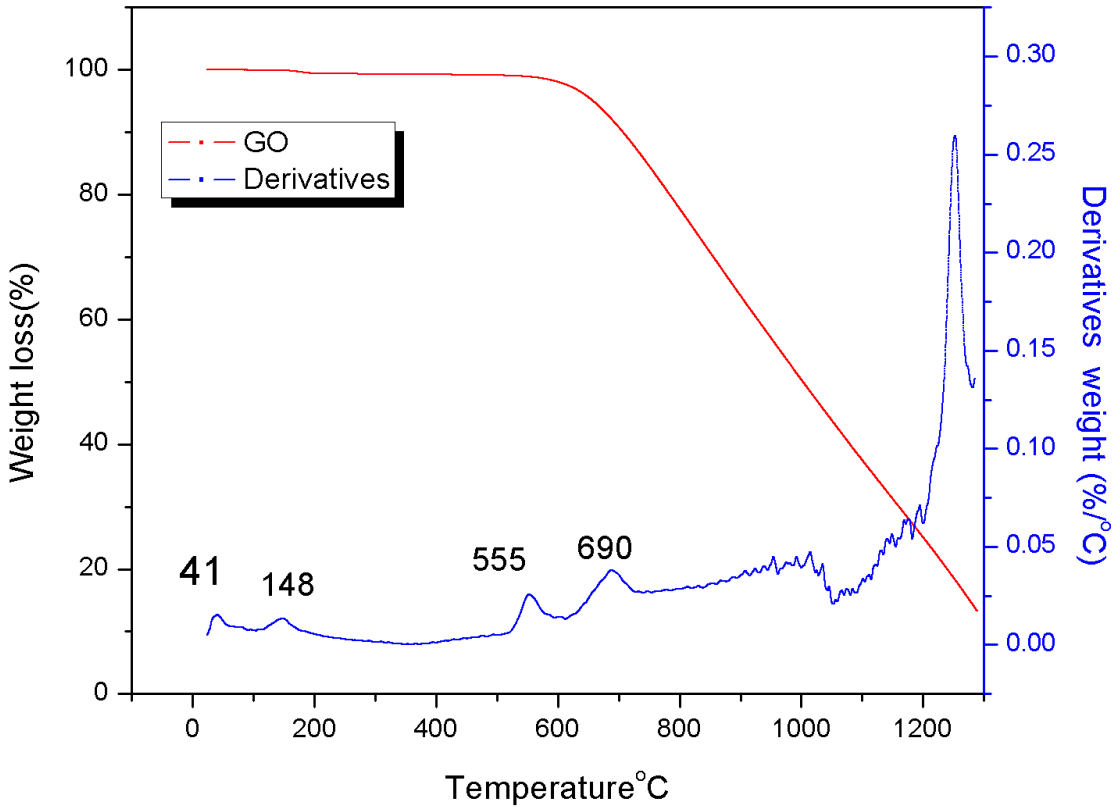

Figure 4.23. TGA of GO with derivatives weight (%/°C)

It was observed on Fig 4.7 that GO is thermally unstable and starts to lose mass due to the desorption of physically adsorbed water when heating even below 100 °C, and there are two significant drops in mass around 226 and 541°C. This decomposition of the labile oxygen-containing functional groups, yielding CO, CO_2, and steam and the latter is attributed to pyrolysis of the carbon skeleton of GO.

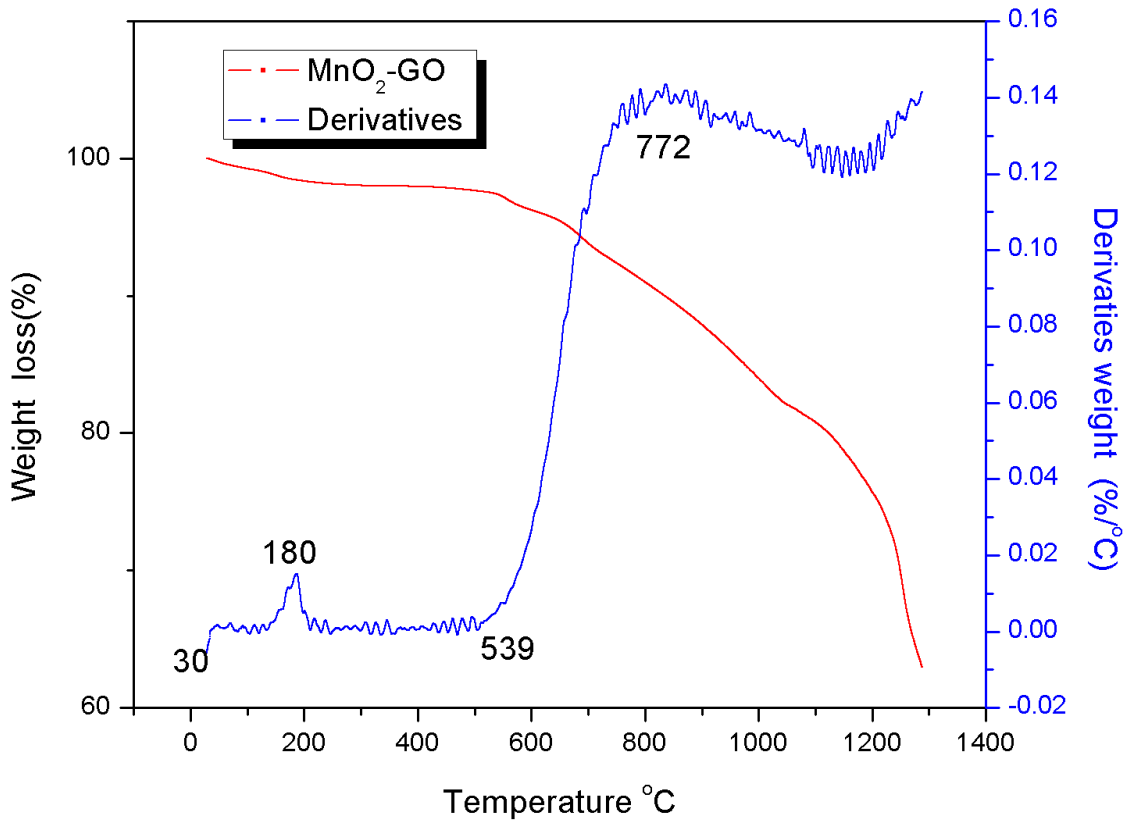

Figure 4.24. TGA curves showing α-MnO_2 with GO and their derivatives

4.4. Branauer Emmett Teller (BET)

The surface areas and equivalent pore size distribution of the α-MnO_2 are determined by measuring nitrogen adsorption–desorption isotherms at 77 K shown in Fig 4.8. The BET surface area of the α-MnO_2 is 134.61 m^2/g and this result obtained can be compared with other results been obtained by other methods used to synthesize MnO_2 [93, 94]. The pore size distribution calculated by Barret–Joyner–Halenda (BJH) method is confirmed by the corresponding pore size distributions (Fig 4.8), which reveals that the existence of mesopores and micropores in α-MnO_2 with a major pore diameter of 1.42 nm. The surface area and porosity of the MnO_2 have a great significant impact on the electrochemical properties of the material.

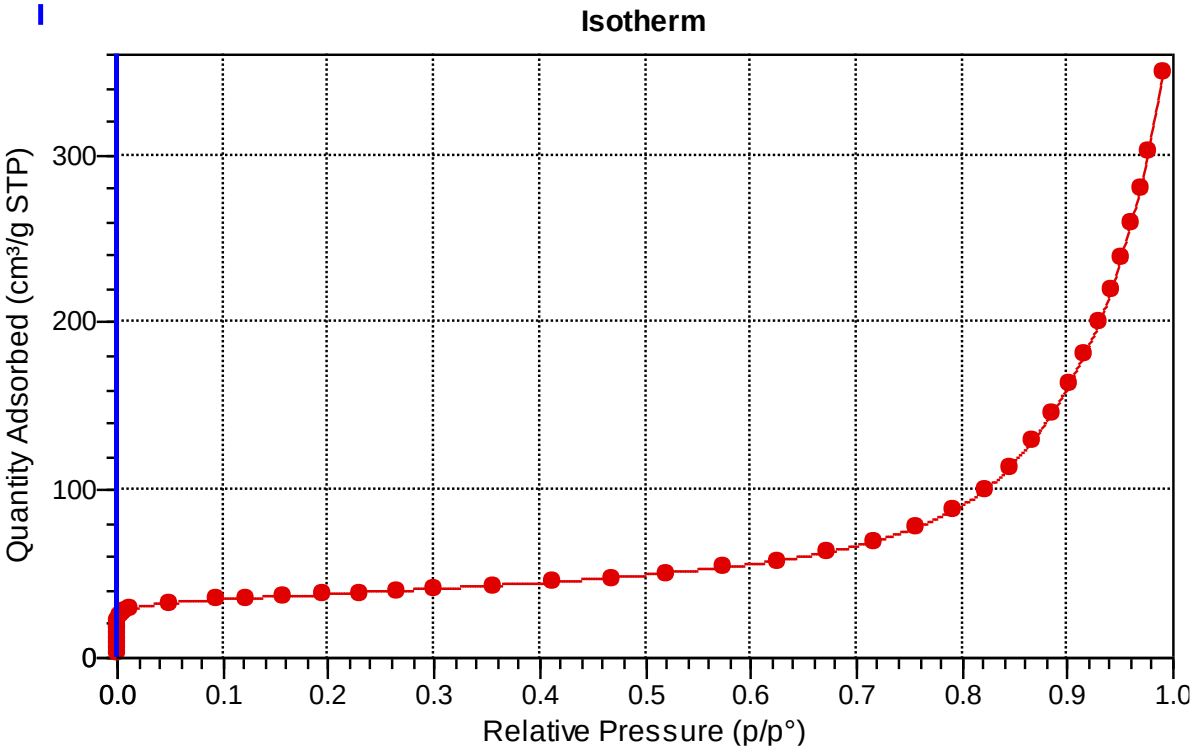

Figure 4.25. N_2 adsorption-desorption isotherms (a) and the corresponding pore distribution

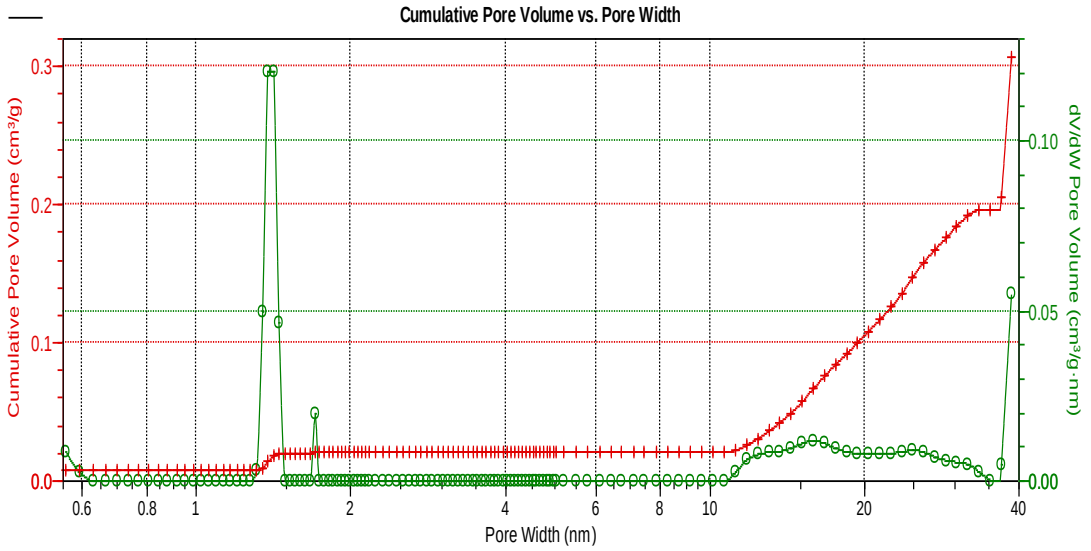

Figure 4.26. N_2 adsorption-desorption isotherms (b) for α-MnO_2 synthesized

4.5. Scanning Electron Microscopy (SEM)

The low and high magnification surface morphology of α-MnO_2 synthesized by microwave–hydrothermal is shown in Fig. 4.10. Fig. 4.10(a) shows homogeneous α-MnO_2 nanospheres structure with a length range from hundred nanometer and numerous micrometer. The microwave irradiation results makes the MnO_2 lattice increase to vibrate and increases MnO_2 mutual repulsion accordingly, that prevents MnO_2 nanospheres from growing and agglomerating.

From Fig 4.10(b), it can be observed that GO layered structure, which exhibit ultrathin and homogeneous GO films. Such films are either crumpled or continuous at times and it is possible to differentiate the boundaries of single sheet, together with kinked and wrinkled areas.

From Fig. 4.10(c) shows morphology images of α- MnO_2-GO materials characterized by SEM. When GO is spread, the composite of α- MnO_2 starts to anchor on GO nanosheet and the content of GO increase which leads to α-MnO_2 decorated on the GO nanosheets. Furthermore, this good contact is also helpful to increase conductivity of the electrode material.

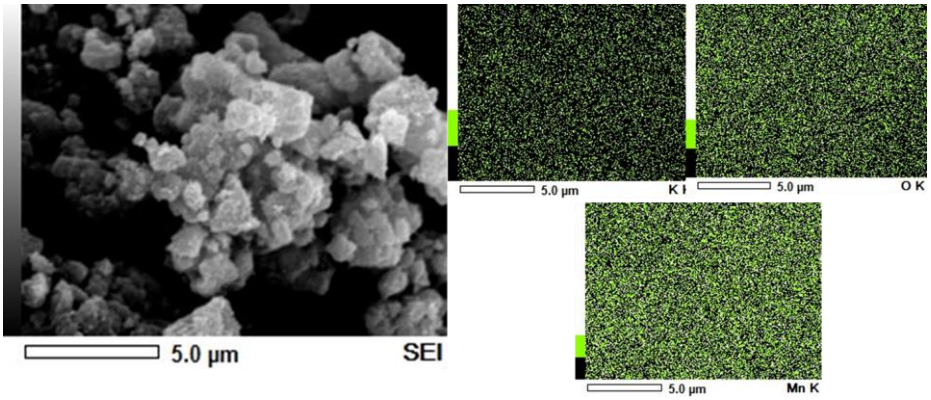

(a)

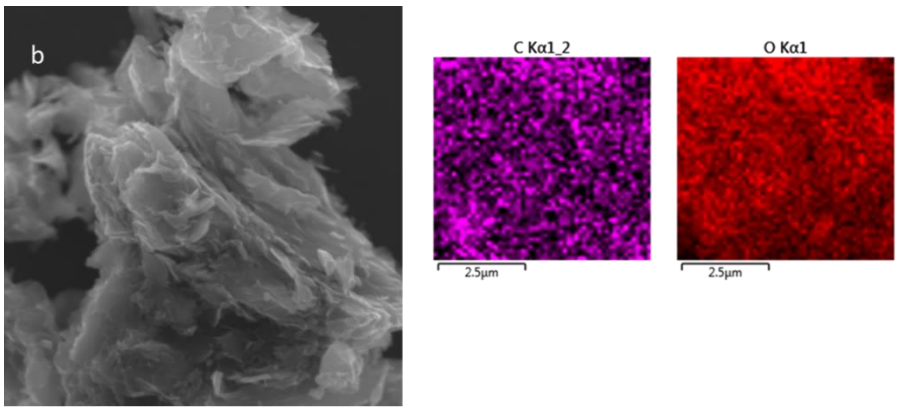

(b)

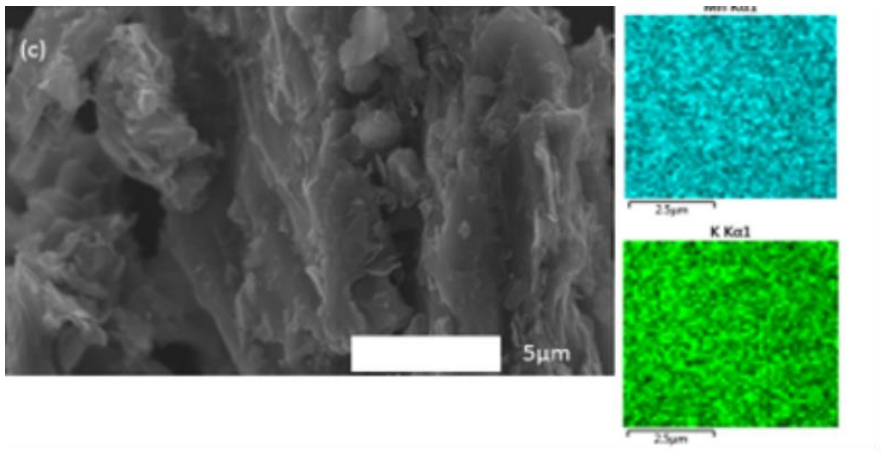

(c)

Figure 4.27. SEM image of MnO_2 synthesised and GO: (a) α-MnO_2 , (b) GO and (c) GO-MnO_2

The EDS analysis was used to study the elemental distribution of α-MnO_2. Fig 4.10a shows the spectroscopy of synthesized α-MnO_2 material by microwave–hydrothermal method. The spectroscopy shows that the α- MnO_2 sample contained some few traces of the carbon (C) element from coating material (Fig 4.10). The compositions of the electrode material synthesised under microwave–hydrothermal conditions are presented in Table 4.1.

Table 4.1. Elemental compositions study obtained with EDS

Elements	Weight%	σ
Mn	54.4	0.2
K	35.1	0.3
O	12.5	0.1

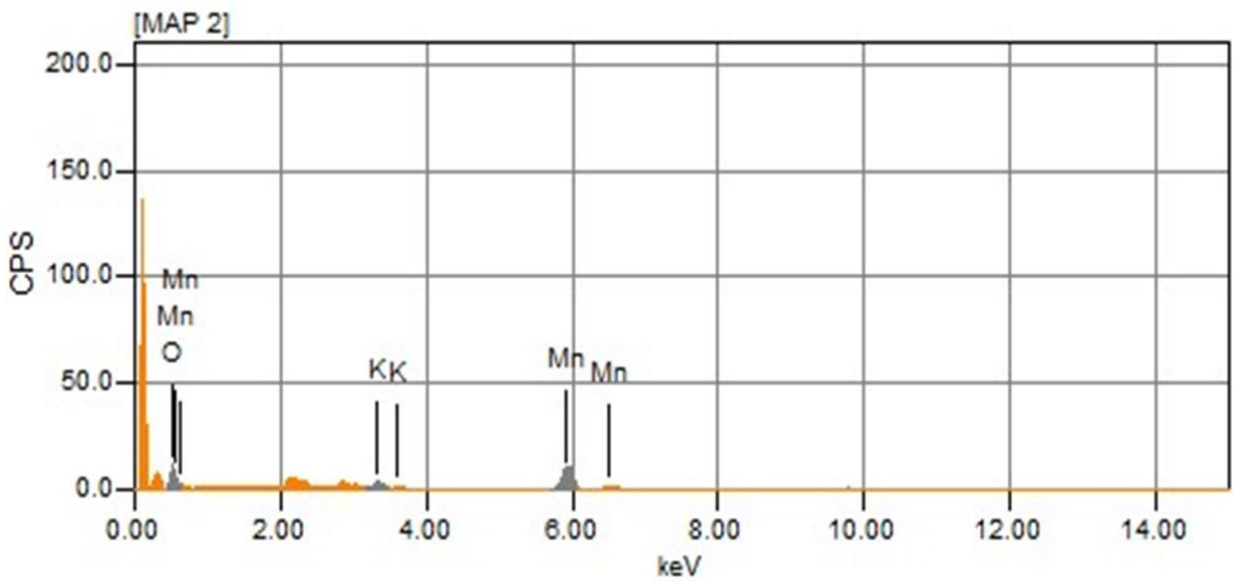

Figure 4.28. The EDS spectroscopy of α-MnO_2

4.6. Electrocatalytic activity of α-MnO_2-GO modified GCE

Electrochemical properties of nanocomposite α-MnO_2 and α-MnO_2-GO studied using CV. The CV test done in a solution of 0.1MKCl containing of 2mM $K_3[Fe(CN)_6]$ and was performed at different scan rate and the voltammograms were obtained. A potential window of -0.2–0.6 V used and results shown below.

Figure 4.12, shows the cyclic voltammograms (CVs) of the α-MnO_2 at different scan rates. The cyclic voltammograms results shows rectangular shape with a symmetric anodic and cathodic half. These CV curves of α-MnO_2 exemplify the ideal pseudocapacitive nature. The mass of MnO_2 at the same scan rate must be due to the kinetics of ions and electrons in the electrode. The CV current density increases slowly with increase of the scan rate of CV. The current density shows attribution to a high porosity and greater surface area [95].

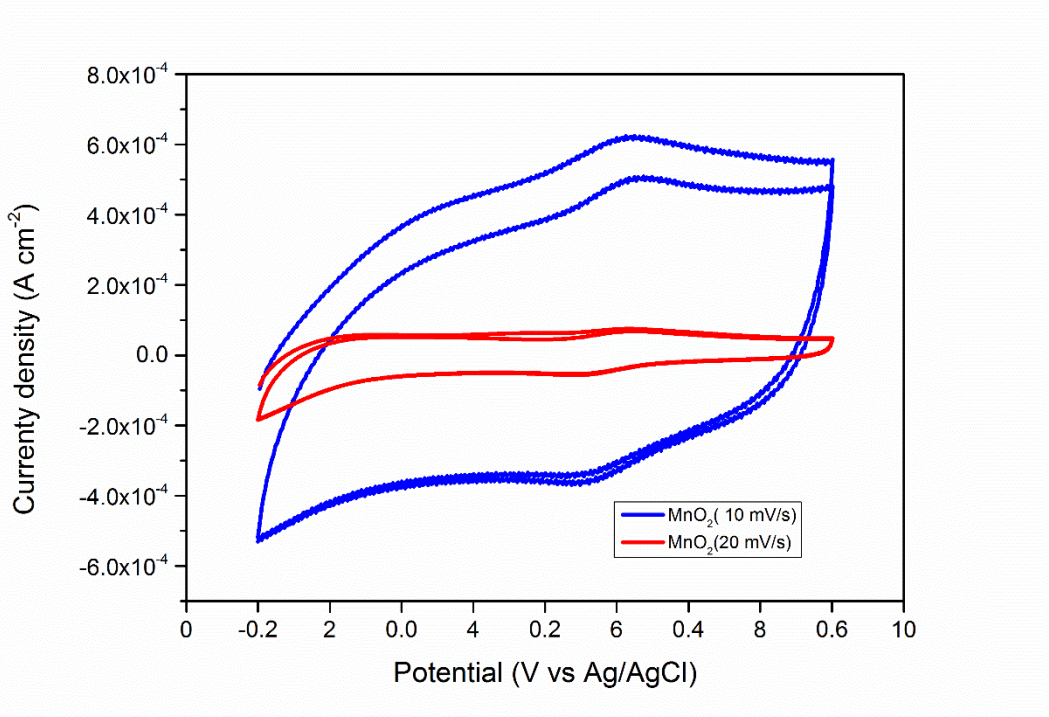

Figure 4.29. CV for α-MnO_2 at scan rate of 10 $mVs^{-1}$and 20mVs^{-1}

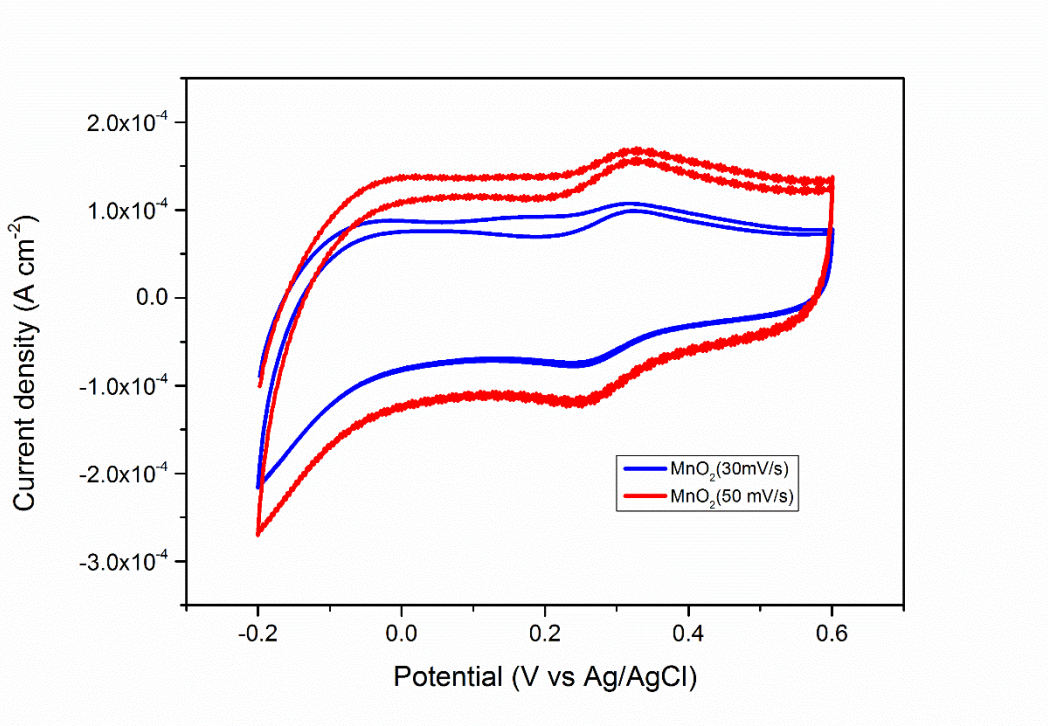

Figure 4.30. CV for α-MnO_2 at scan rate of 30 $mVs^{-1}$and 50 mVs^{-1}

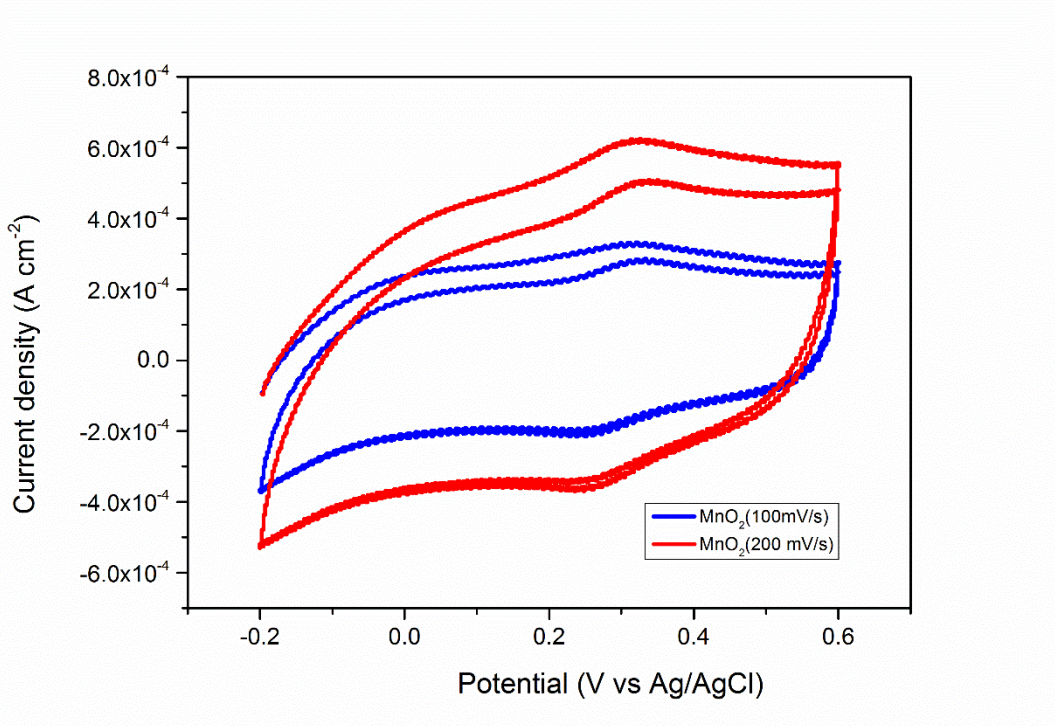

Figure 4.31. CV for α-MnO_2 at scan rate of 100 mVs^{-1} and 200mVs^{-1}

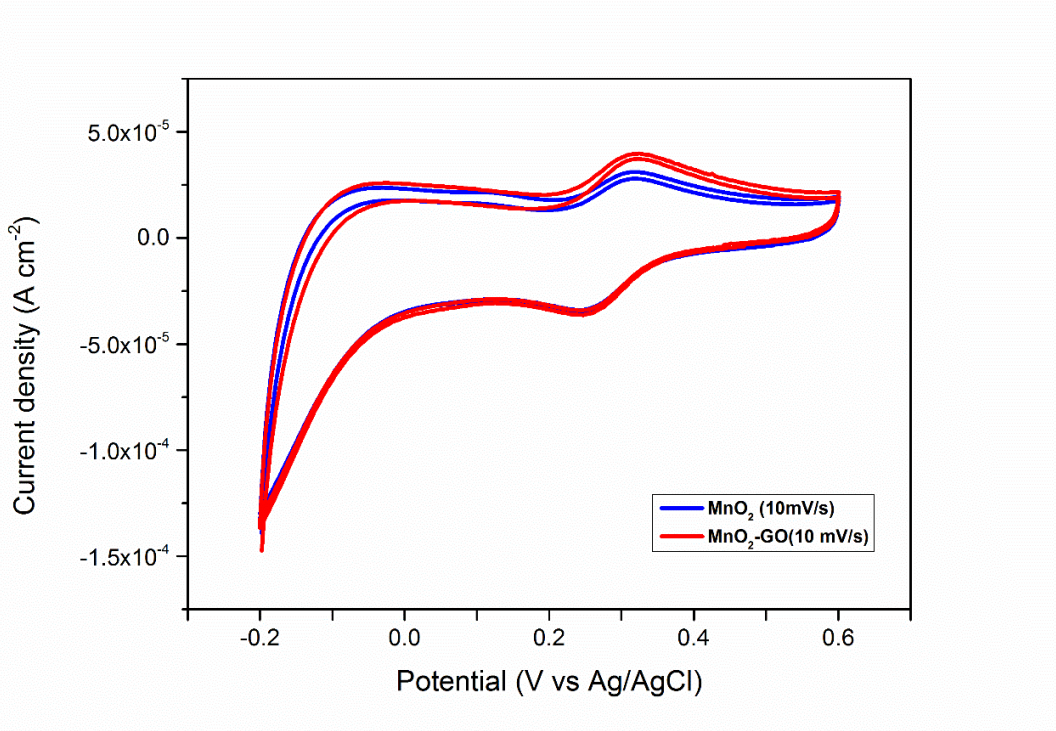

Figure 4.32. CV for α-MnO_2-GO and MnO_2 at scan rate of 10 mVs^{-1}

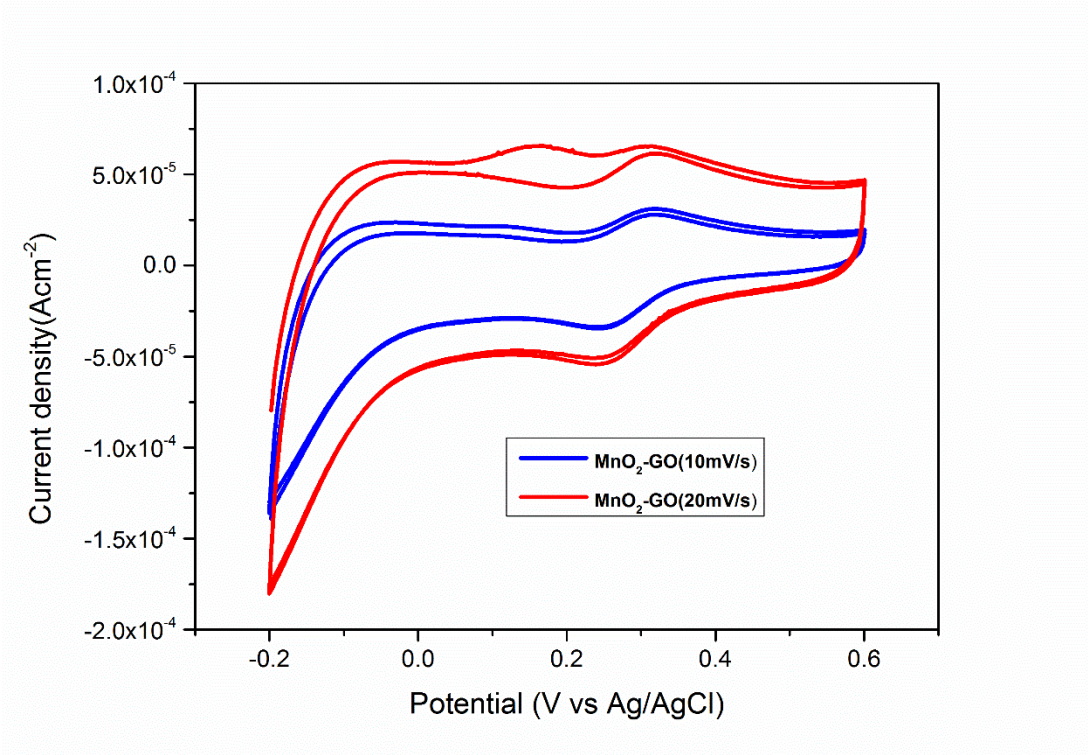

Figure 4.33. CV for α-MnO_2-GO at scan rate of 10 mVs^{-1} and 20mVs^{-1}

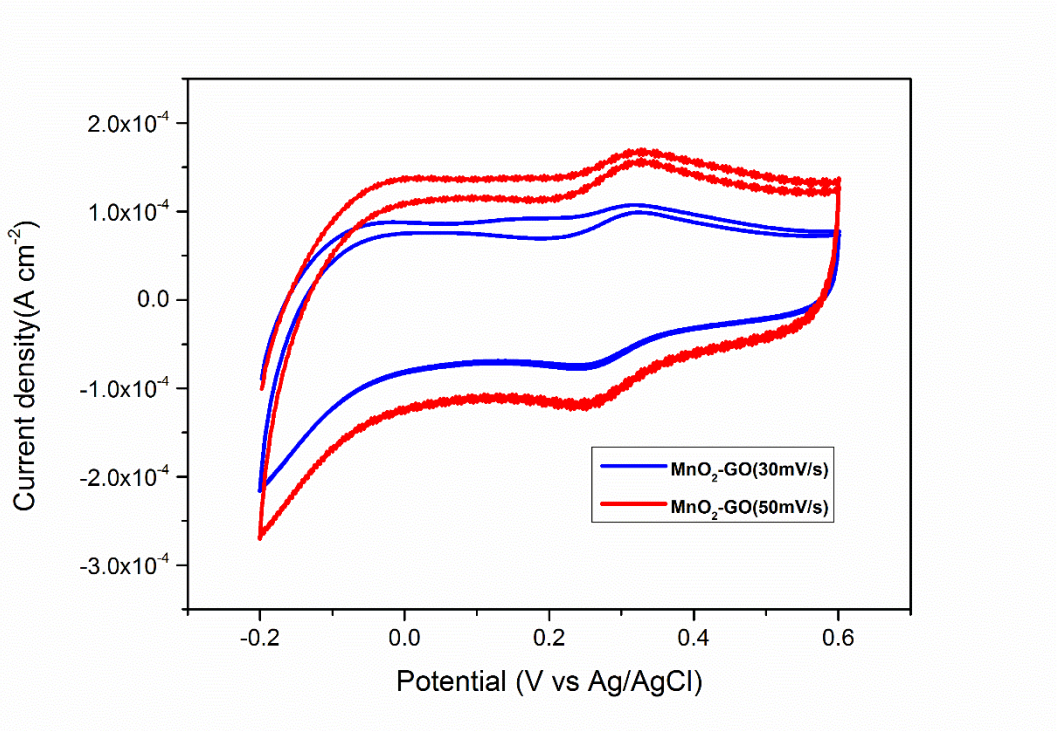

Figure 4.34. CV for α-MnO_2-GO at scan rate of 30mVs^{-1} and 50mVs^{-1}

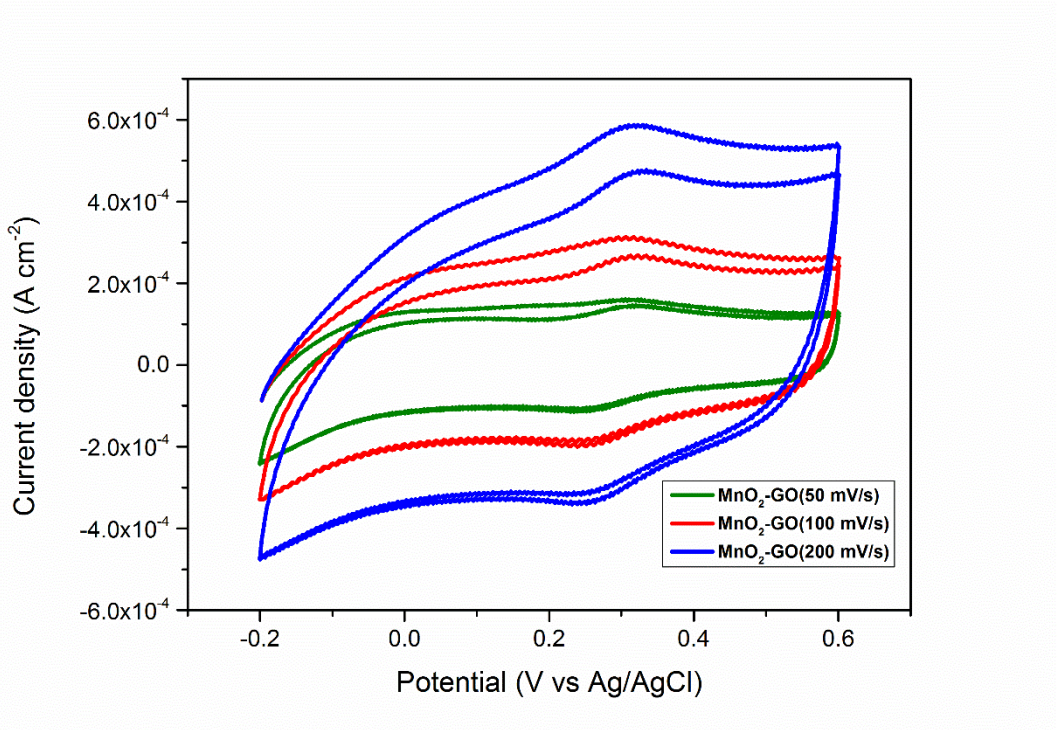

Figure 4.35. CV for α-MnO_2-GO at scan rate of 50mVs^{-1},100 mVs^{-1} and 200mVs^{-1}

Figure 4.12 shows the cyclic voltammograms (CVs) of the α-MnO_2-GO at different scan rates. Fig. 4.13 shows the cyclic voltammetric (CV) results current response increased accordingly, the shape of the CV curve indicates good rate performance. Fig. 4.14 showing better performance with high current response. The redox reactions mostly depend on the presence of the alkali ion or protons from the electrolyte [96]. At slower scan rates, the diffusion of ions from the electrolyte can gain access to almost all available pores of the electrode. Fig. 4.15 and Fig11.16 demonstrate quasi-rectangular shapes and symmetric shape with cycling stability. When the scan rate is higher, the effective utilization for the redox reaction is limited only to the outer surface of α-MnO_2 electrode. Infect the surface area will greatly influence the catalytic activity if is either high or low [92] .The other reflection is that α-MnO_2 nanostructures give more positive onset potential a larger peak current, which clearly indicate the superior electro catalytic activity of α-MnO_2. The CV curves remain in the almost ideal rectangular shape, implying that this α-MnO_2 phase have good pseudo-capacitor properties [97].

The CV curves of all scan rates have rapid current response at the switching potential at both ends in forward and reverse scans. Moreover, the α-MnO_2-GO materials have ideal capacitive behavior and with small amount of GO incorporated increases the specific capacitance. The presence of a cathodic current peak for oxygen reduction can be assigned to the electrocatalytic activity of the as-synthesized α-MnO_2 [61]. To evaluate the electrocatalytic performance of all scan rates for α-MnO_2 and GO, the onset potential, peak current, and potential are given in table 4.2 and 4.3.

Table 4.2. Onset potential and current peak for α-MnO_2 on 2mM ferricyanide ($K_3Fe(CN)_6$.) in KCl

Scan rate	**MnO_2**				**2mM ($K_3Fe(CN)_6$.)**	
	Ipa	**Ipc**	**Epa**	**Epc**	**ΔE=Ea-Ec**	**Epa/Epc**
10mV/s	4.12×10^{-5}	5.55×10^{-5}	0.31103	0.2531	0.56413	0.743555
20mV/s	7.68×10^{-5}	5.55×10^{-5}	0.32208	0.25588	0.0662	1.38455
30mV/s	1.09×10^{-4}	7.77×10^{-5}	0.3252	0.2727	0.0525	1.39746
50mV/s	1.71×10^{-4}	1.71×10^{-4}	0.31695	0.2534	0.06355	1
100mV/s	3.25×10^{-4}	2.12×10^{-4}	0.3083	0.26138	0.04692	1.52923
200mV/s	6.31×10^{-4}	3.61×10^{-4}	0.31933	0.25313	0.0662	1.7495

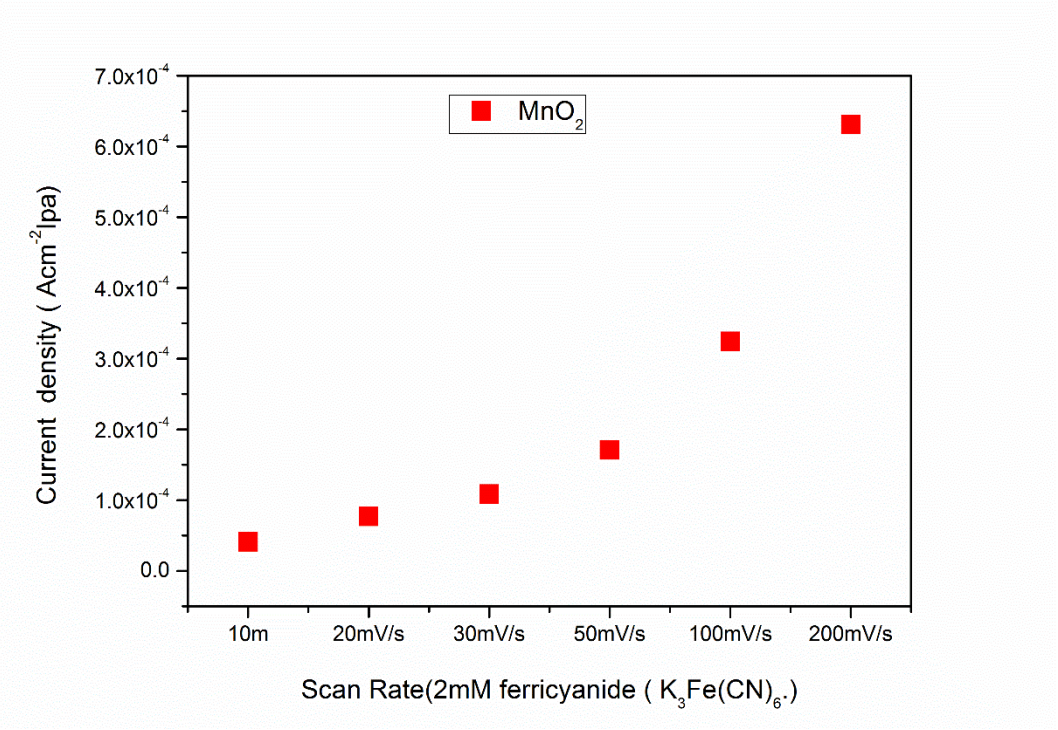

Figure 4.36. Current peak and Scan rate for α-MnO_2 on 2mM $K_3Fe(CN)_6$.) in KCl

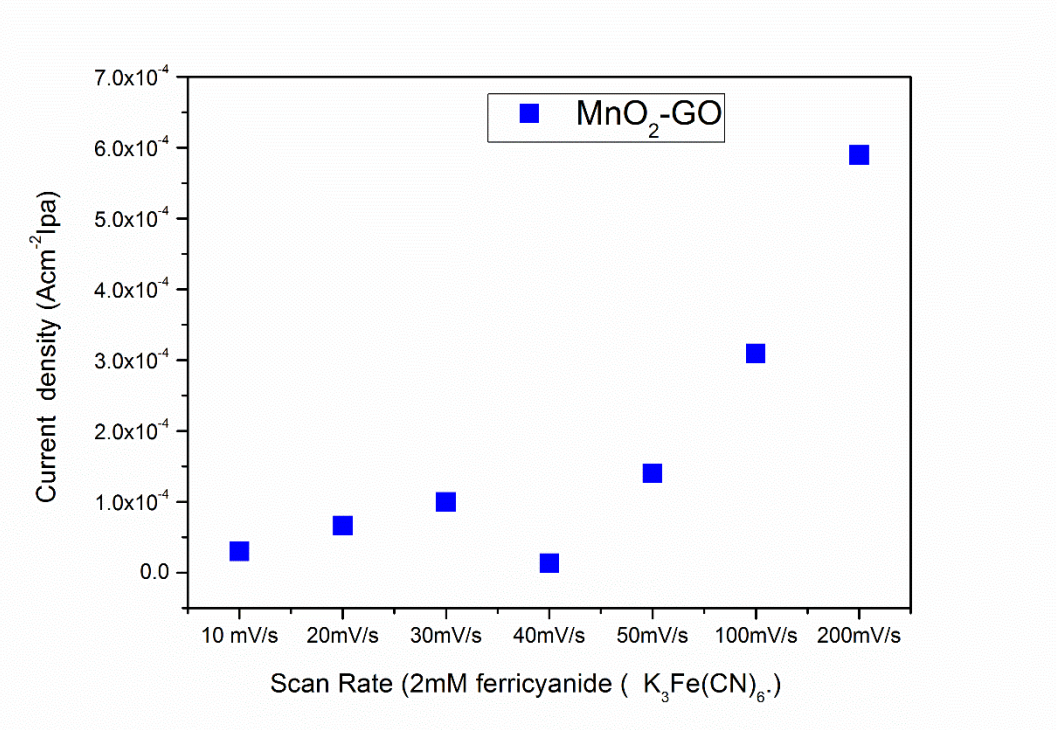

Figure 4.37. Current peak and Scan rate for α-MnO_2-GO on 2mM ($K_3Fe(CN)_6$.) in KCl

Table 4.3. Onset potential and current peak for α-MnO2 –GO on 2mM ($K_3Fe(CN)_6$.) in KCl

Scan rate	**α-MnO_2**				**2mM ($K_3Fe(CN)_6$.)**
	Ipa	**Ipc**	**Epa**	**Epc**	**ΔE=Ea-Ec**	**Epa/Epc**
10mV/s	3×10^{-5}	3.16×10^{-5}	0.31133	0.2448	0.55613	0.9490442
20mV/s	6.63×10^{-5}	5.6×10^{-5}	0.31193	0.24764	0.064293	1.1897418
30mV/s	9.97×10^{-5}	6.76×10^{-4}	0.31695	0.26174	0.05521	0.147629
40mV/s	1.31×10^{-5}	7.99×10^{-4}	0.30297	0.24799	0.05498	0.0163479
50mV/s	1.4×10^{-4}	8.11×10^{-3}	0.3114	0.25624	0.05521	0.0172551
100mV/s	3.09×10^{-4}	2.03×10^{-4}	0.300229	0.25899	0.041239	1.5263072
200mV/s	5.89×10^{-4}	3.41×10^{-4}	0.3057	0.25349	0.05221	1.7305948

4.7. The utilization of α-MnO_2-GO on MFCs.

The overall aim of this research is to design a dual chamber MFC and investigate the effect of introducing α-MnO_2-GO electro-catalysts material on the MFC performance. Municipality sewage wastewater will be utilized as a fuel source to explore the possibility of generating electricity and producing clean water simultaneously. Wastewater is also known as one of the main contributing factors for environmental pollution. The earlier studies have demonstrated various wastewater as substrates and their potential for a sustainable to mitigate the growing energy demands[10, 24].

The initial work of MFC were carried out on laboratory scale studies and usually functioned in continues mode using a dual-chamber configuration. Among other challenges that restrict high power generation on dual chamber were electron acceptor limitations and higher internal resistance. However, the resent trend research involves a single-chambered MFCs reporting maximum power density up to 26 mW /m^2 with up to 80% chemical oxygen demand (COD) removal whereby domestic wastewater used as substrate with COD ranging between 200–300 mg/l [98].

An advance in the design of the dual chamber MFC in terms of architectural and material of construction may overcome all the limitation. In addition over the years 4200 mW/m^2 power densities in MFCs is reached with up to 100% COD and other contaminants removal. In this study, rectangular constructed dual chamber MFC with anode graphite electrode, coated with electro catalysts MnO_2-GO cathode electrode separated by a Nafion 117 membrane for proton transfer was develop, and tested to energy generation from municipality sewage wastewater**.** The two electrodes were connected with copper wire through a resistor ranging from 1.0 to 550 Ω.

4.7.1. Wastewater Analysis Result

The wastewaters were analysed to observe their suitability to act as electrolyte in anode chambers of MFCs. The characteristics of the wastewaters were observed as shown in Table 4.4

Table 4.1. Characterization of different wastewaters sample

Daspoort municipality sewage wastewater					
Daspoort wastewater	Cycle1	Cycle 2	Cycle 3	Cycle 4	Cycle 5
pH	6.88	7.33	5.89	4.12	6.71
COD (mg/L)	287	291	155	136	211
Conductivity (mS/cm)	2.28	6.67	5.84	6.11	2.14
Temperature ^oC	19.5	20.7	21.1	20.1	18.85

4.7.2. MFC performance

In this experiment, a cathode electrode coated with 20 $mg.cm^{-2}$ of MnO_2-GO electro-catalysts and 50 mM of ferricyanide medium feed been used. MFC will operated under continuous mode at hydraulic retention time (HRT) of 20 h for 10 days. The maximum voltage of 586 mV was reached during MFC operation even though the leakage occurs in between anode and cathode. This high voltage could be subjective essentially by electrochemical factors between the anode and the cathode due to potential difference. After 3 days of incubation with municipal

sewage wastewater, the stable voltage value of 390 ± 35 mV was obtained on the third feeding cycles. The MFC operation cycle was under open circuit voltage over 240h. The leakage on the anodic chamber have great impact on voltage decreased from 586 mV to 101 mV. The municipality wastewater replaced when the voltage reached below 100mv. The differences voltage between anode and cathode were observed throughout the biofilm formation. This results are similar to previous studies depends on wastewater concentration [99].

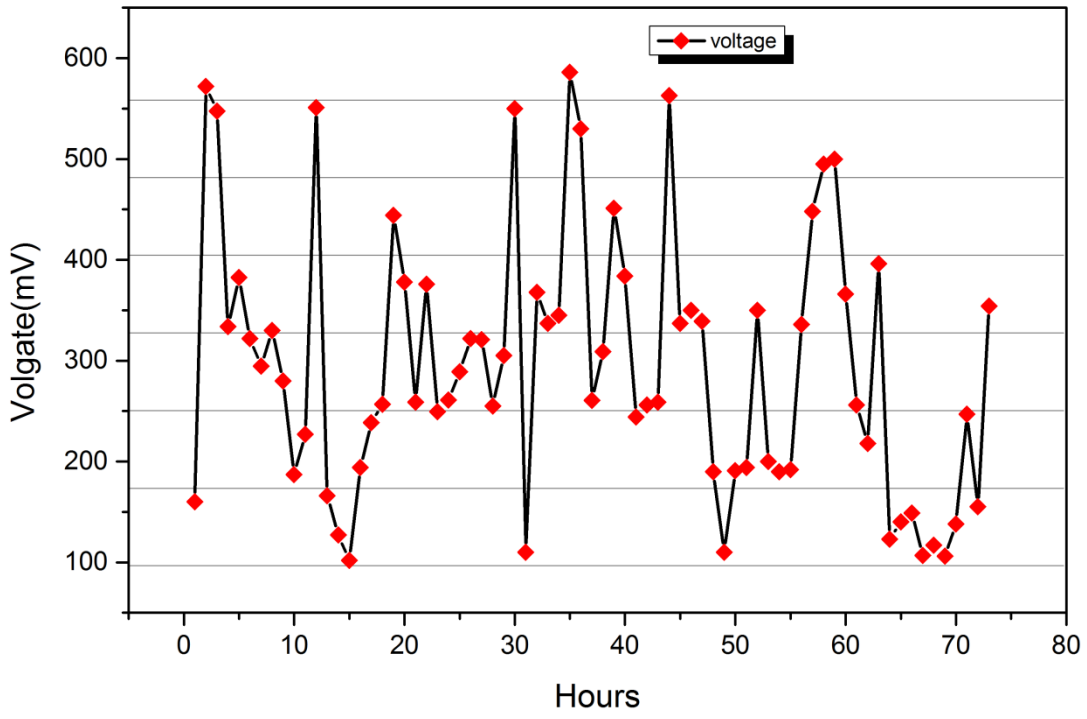

Figure 4.38. Deviation of Potential Difference with time

4.7.3. Continuous power generation

Figure 4.21 shows the polarization curves obtained with different external resistances ranging between 1 to 550 Ω during all experimental periods. However, dual-MFC reactor employed various sewage municipal wastewater COD (100-300mg/L) and operate for 10 days (240 hours) to determine the maximum power output. The decreasing current generated trend with increasing resistance was detected. The low resistances under fuel cell circuit allow more

electrons to flow and to neutralize the protons (H^+) existing at the cathode, in comparison to higher resistance, which resulted in rapid stabilization of potential at higher resistances.

The maximum power density of 248 mW/m^2 with resistance of 16.98 Ω and highest current density of 1.72mA/m^2 was observed at the first cycle as compare to other cycle. The lowest value of 0.002159 mA/m^2 obtained at the end of 10 days. MFC displayed instable trend in the voltage as well as current response during the experiments. In some previous studies, the high COD concentration substrate increased power density in MFCs. In some earlier studies, MFC power generation depends also on wastewater concentration and this finding is consistent.

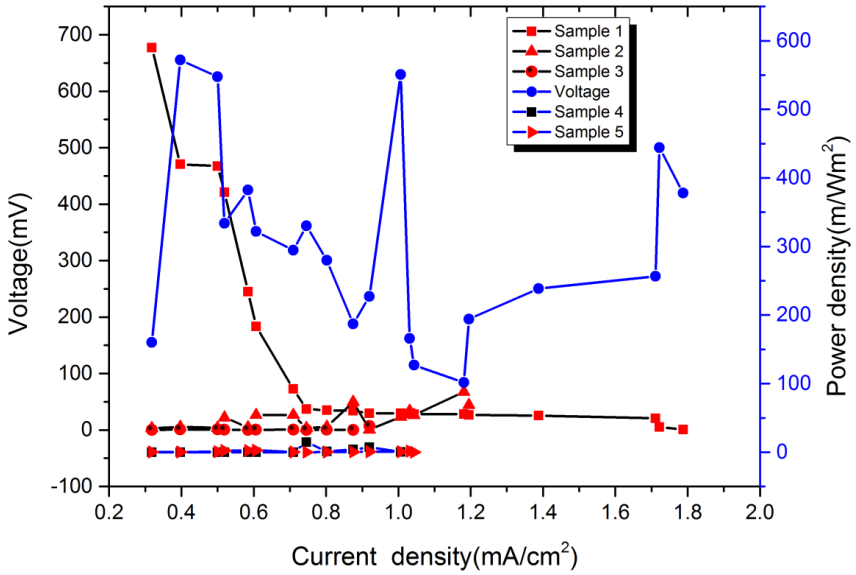

Figure 4.39. Polarization curve and Power density for MFC on four cycle.

■ Power Density ● Potential Difference

The open circuit voltage (OCV) of four cycle indicate maximum power density and maximum current output measured at different point by changing external resistance from 1 to 600Ω. The results obtained for OCV were consecutively at 304 mV for first cycle, 341 mV for second cycle, 379 mV for the third cycle and 205 mV for fourth cycle**.** These findings confirm results in the literature [100].

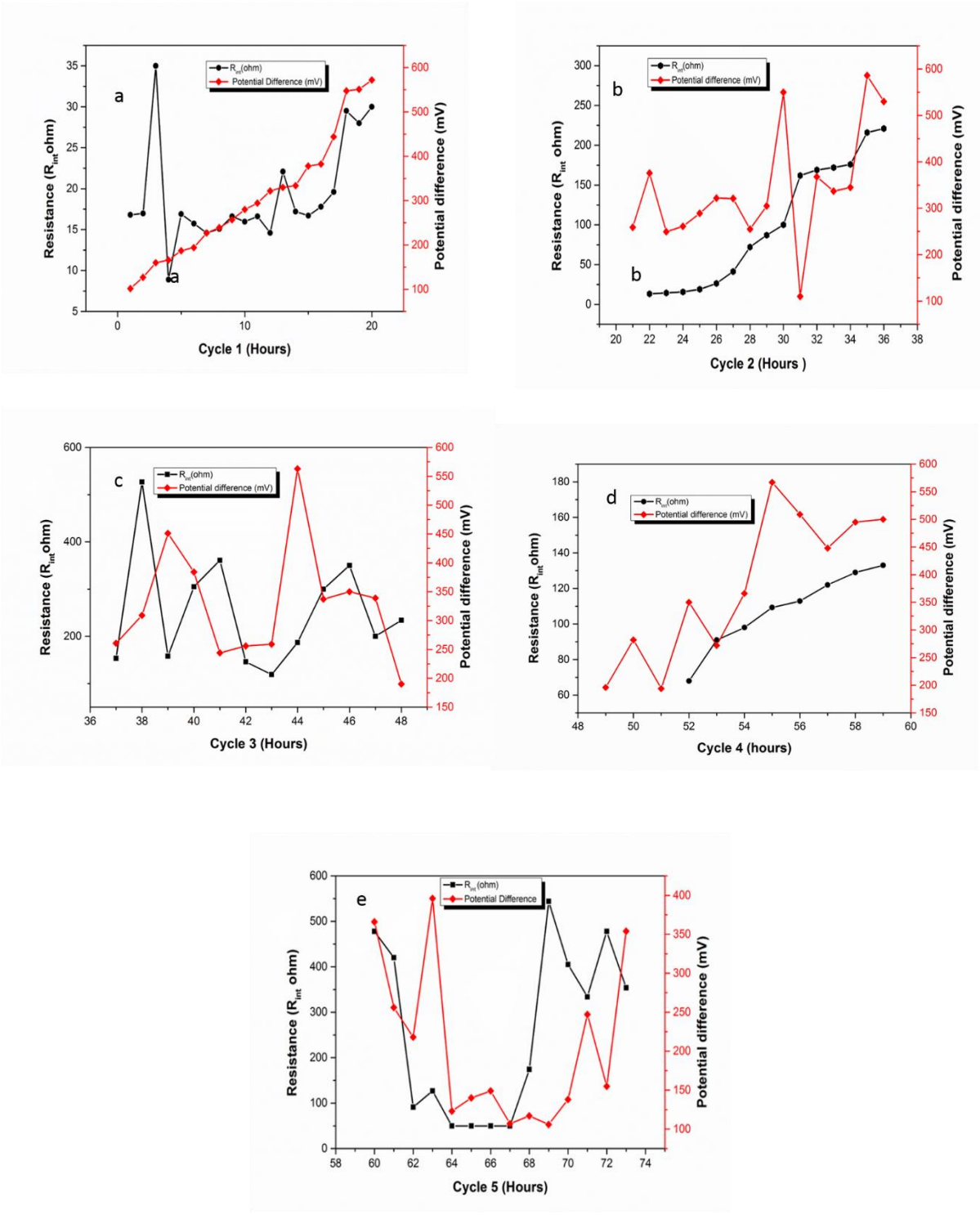

Figure 4.40. External resistance during first cycle, second cycle, third cycle, fourth cycle and fifth cycle related to potential difference

The relationship between resistance and COD concentration with time contributing to potential difference as indicated (Fig4 .23.). Low variance external resistance recorded in the first cycle, in second cycle increase greatly at 36 hours and further increase with time occurs in third and fifth cycle. Fourth, cycle also exhibit lower resistance as compare to other cycle.

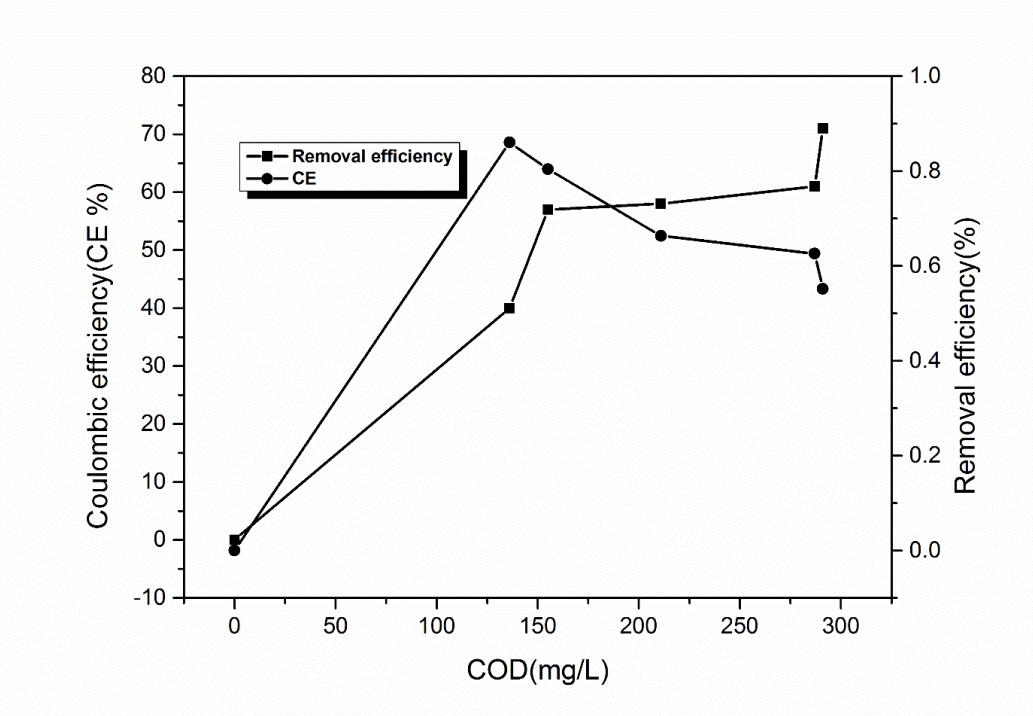

Figure 4.41. COD concentrations, organic removal efficiencies, and Coulombic efficiency

Coulombic efficiency, used often to describe MFC systems efficiency and all four cycles of MFC were calculated including the COD removal efficiency as shown in Figure 4.24. The data showed that there is a proportional relationship between COD removal and CE. Firstly, the COD removal efficiency was very low, as was the CE of the system, but a substantial increase in both parameters was found as the cycle continued. The high COD removal was attributed to the long operation period, which also extended the time for oxygen diffusion into the system, because of low CE. Higher CE increased COD removal. The highest COD removal efficiency achieved was 71% at an influent COD of 291 mg/L. It was observed that as the power increased at highest of 248 m/Wm^2 but the coulombic efficiency decreased with lowest of 0.57%.

4.7.4. Conclusions

Relatively low-cost catalyst α-MnO_2-GO was used on constructed dual-chamber MFC for energy generation were much higher than those previously obtained using low strength wastewater. Generally, cathode fouling and membrane leaks had great impact on power decreasing. The distance between anode and cathode determine the output voltage produced during operation [101].

4.8. References

[1] N. Sui, Y. Duan, X. Jiao, D. Chen, Large-Scale Preparation and Catalytic Properties of One-Dimensional α/β-MnO_2 Nanostructures, The Journal of Physical Chemistry C, 113 (2009) 8560-8565.

[2] D.C. Marcano, D.V. Kosynkin, J.M. Berlin, A. Sinitskii, Z. Sun, A. Slesarev, L.B. Alemany, W. Lu, J.M. Tour, Improved Synthesis of Graphene Oxide, ACS Nano, 4 (2010) 4806-4814.

[3] W.S. Hummers, R.E. Offeman, Preparation of Graphitic Oxide, Journal of the American Chemical Society, 80 (1958) 1339-1339.

[4] Y.X. Zhang, M. Huang, F. Li, X.L. Wang, Z.Q. Wen, One-pot synthesis of hierarchical MnO2-modified diatomites for electrochemical capacitor electrodes, Journal of Power Sources, 246 (2014) 449-456.

[5] M.G. H.Adelkhani, S.M.Jafari, Novel Nanostructured MnO_2 Prepared by Pulse Electrodeposition: Characterization and Electrokinetics, J. Mater. Sci. Technol., 24 (2008) 857-862.

[6] Z. Li, J. Wang, S. Liu, X. Liu, S. Yang, Synthesis of hydrothermally reduced graphene/MnO_2 composites and their electrochemical properties as supercapacitors, Journal of Power Sources, 196 (2011) 8160-8165.

[7] W. Xiao, D. Wang, X.W. Lou, Shape-Controlled Synthesis of MnO_2 Nanostructures with Enhanced Electrocatalytic Activity for Oxygen Reduction, The Journal of Physical Chemistry C, 114 (2010) 1694-1700.

[8] R.N. Reddy, R.G. Reddy, Synthesis and electrochemical characterization of amorphous MnO_2 electrochemical capacitor electrode material, Journal of Power Sources, 132 (2004) 315-320.

[9] V. Subramanian, H. Zhu, R. Vajtai, P.M. Ajayan, B. Wei, Hydrothermal Synthesis and Pseudocapacitance Properties of MnO_2 Nanostructures, The Journal of Physical Chemistry B, 109 (2005) 20207-20214.

[10] J. Zang, X. Li, In situ synthesis of ultrafine [small beta]-MnO_2/polypyrrole nanorod composites for high-performance supercapacitors, Journal of Materials Chemistry, 21 (2011) 10965-10969.

[11] C.-C. Hu, T.-W. Tsou, Ideal capacitive behavior of hydrous manganese oxide prepared by anodic deposition, Electrochemistry Communications, 4 (2002) 105-109.

[12] M.-W. Xu, D.-D. Zhao, S.-J. Bao, H.-L. Li, Mesoporous amorphous MnO_2 as electrode material for supercapacitor, Journal of Solid State Electrochemistry, 11 (2007) 1101-1107.
[13] S. Chen, J. Zhu, X. Wu, Q. Han, X. Wang, Graphene Oxide−MnO_2 Nanocomposites for Supercapacitors, ACS Nano, 4 (2010) 2822-2830.
[14] V.G. Gude, Wastewater Treatment in Microbial Fuel Cells – An Overview, Journal of Cleaner Production.
[15] S. Burton, B. Cohen, S. Harrison, S. Pather-Elias, W. Stafford, R. Van Hille, H. Von Blottnitz, Energy from Wastewater-a Feasibility study, WRC, South Africa, (2009).
[16] Q. Wen, Y. Wu, L.-x. Zhao, Q. Sun, F.-y. Kong, Electricity generation and brewery wastewater treatment from sequential anode-cathode microbial fuel cell, Journal of Zhejiang University SCIENCE B, 11 (2010) 87-93.
[17] L. He, P. Du, Y. Chen, H. Lu, X. Cheng, B. Chang, Z. Wang, Advances in microbial fuel cells for wastewater treatment, Renewable and Sustainable Energy Reviews, 71 (2017) 388-403.
[18] Q. Wen, Y. Wu, D. Cao, L. Zhao, Q. Sun, Electricity generation and modeling of microbial fuel cell from continuous beer brewery wastewater, Bioresource Technology, 100 (2009) 4171-4175.
[19] S. Srikanth, M. Kumar, D. Singh, M.P. Singh, B.P. Das, Electro-biocatalytic treatment of petroleum refinery wastewater using microbial fuel cell (MFC) in continuous mode operation, Bioresource Technology, 221 (2016) 70-77.

CHAPTER 5

CONCLUSIONS AND FUTURE WORK

5.1.Conclusions

This research reports on the dual chamber MFC design use wastewater (municipal sewage) and electro-catalyst(α-MnO_2-GO) for cathode graphite electrode to generate electricity.The dual chamber MFC consisting of an anode graphite electrode and cathode electrode separated by a Nafion 117 membrane. The role of manganese oxide (MnOx) as an electro catalyst for oxygen reduction reaction (ORR) in the MFC while using reduced graphene (rGO) as a support to enhance electrode surface area. The effect of graphene material loading on MnOx catalyst for electrochemistry. The dual chamber MFC design functioned successfully and tested for energy generation from municipality sewage wastewater. The maximum voltage of 586 mV reached during MFC operation with various sewage municipal wastewater COD of 100-300mg/L. The maximum power density of 248 mW/m^2 with resistance of 16.98 Ω and highest current density of 1.72mA/m^2 was observed at the first cycle as compare to other cycle. The lowest value of 0.002159 mA/m^2 obtained at the end of 10 days. The content of municipality sewage wastewater is capable of generating electricity.

The physico-chemical properties of α-MnO_2 exhibits excellent cycling stability on the electrochemical. This excellent cycling stability of α-MnO_2 as a super capacitor electrode material. In addition, the graphene material loading on α-MnO_2 has improved the electro catalytic activity, which influences the kinetics of the reduction reaction. MFC technology has the potential to finds its own niche in the energy industry as it is becoming more and more sustainable due to the lower cost of electro catalyst materials. Power densities of 248 mW/m^2 using wastewater with COD of 291mg/l were much higher than those previously obtained using low strength wastewater.

5.2.Future work

These results have opened doors for further investigation of improving electro catalysis, utilized high concentration wastewater with high COD and improved MFC design including cheap electrode materials. Generally, cathode fouling and membrane leaks had great impact on power decreasing. The distance between anode and cathode need be relooked. MFCs possess a unique feature in the field of fuel cell and more focus needed on high-quality structures for real commercialization scale application.

Although studies have shown, microwave-hydrothermally preparation of α-MnO_2 as a good electrocatalyst material for energy storage the quality of α-MnO_2 still needs to improved due to agglomeration. It is also important to understand fully the electrochemical behavior on the electrodes. In addition to three electrode and symmetric configuration and a symmetric configuration is recommended in order to increase the working potential and capacitance.
Loading (rGO) material on MnO_2 catalyst is also recommended. Optimization of design factors such as brush length, diameter, orientation and number of brushes will likely further decrease the internal resistance and increase power. Furthermore, structural and supporting material used in reactors needs to be designed in such a way that it does not reduce mass transfer to and from electrode surfaces.

There has been substantial progress towards scale-up and practical application of MFC technology in the last decade. However, to date, there are still many obstacles to overcome. Primarily, a successful pilot-scale study, demonstrating the feasibility MFC technology for practical application, is paramount. In the near future, a greater focus on scaling-up flatplate designs will likely lead to significant advances in taking this technology from the laboratory to the pilot scale and beyond. Additionally, wastewater streams with high organic concentrations is recommended as suitable for energy generation. Further studies that investigate other media such as permanganate as the cathode electron acceptor should be conducted.